



**STUDY OF COEXISTENCE OF
SUPERCONDUCTIVITY AND
ANTIFERROMAGNETISM IN $\text{SmAsO}_{1-x}\text{F}_x\text{Fe}$**

By
ABERA MEBRAHTU

SUBMITTED IN PARTIAL FULFILLMENT OF THE
REQUIREMENTS FOR THE DEGREE OF
MASTER OF SCIENCE IN PHYSICS

AT
ADDIS ABABA UNIVERSITY
ADDIS ABABA, ETHIOPIA

JUNE 2011

ADDIS ABABA UNIVERSITY
DEPARTMENT OF
PHYSICS

Supervisor:

PROF.P SINGH

Examiners:

PROF.Malnev

Dr.Chernet

ADDIS ABABA UNIVERSITY

Date: **JUNE 2011**

Author: **ABERA MEBRAHTU**

Title: **STUDY OF COEXISTENCE OF
SUPERCONDUCTIVITY AND
ANTIFERROMAGNETISM IN $\text{SmAsO}_{1-x}\text{F}_x\text{Fe}$**

Department: **Physics**

Degree: **M.Sc.** Convocation: **JUNE** Year: **2011**

Permission is herewith granted to Addis Ababa University to circulate and to have copied for non-commercial purposes, at its discretion, the above title upon the request of individuals or institutions.

Signature of Author

THE AUTHOR RESERVES OTHER PUBLICATION RIGHTS, AND NEITHER THE THESIS NOR EXTENSIVE EXTRACTS FROM IT MAY BE PRINTED OR OTHERWISE REPRODUCED WITHOUT THE AUTHOR'S WRITTEN PERMISSION.

THE AUTHOR ATTESTS THAT PERMISSION HAS BEEN OBTAINED FOR THE USE OF ANY COPYRIGHTED MATERIAL APPEARING IN THIS THESIS (OTHER THAN BRIEF EXCERPTS REQUIRING ONLY PROPER ACKNOWLEDGEMENT IN SCHOLARLY WRITING) AND THAT ALL SUCH USE IS CLEARLY ACKNOWLEDGED.

Table of Contents

Table of Contents	v
List of Figures	vi
Abstract	vii
Acknowledgements	viii
1 Introduction	1
2 Literature Review	4
2.1 Meissner effect	4
2.2 Types of superconductors	5
2.3 Phenomenological and BCS theory	6
2.4 High Temperature Superconductivity and its Mechanism	7
2.5 Superconductivity and Magnetism in Fe-pnictide Superconductors	10
2.6 Crystal Structure of Fe-pnictide Superconductors	12
2.7 Physical Properties $R(O_{1-x}F_x)FeAs$	13
2.8 Mechanism of superconductivity in Fe-pnictide	15
2.8.1 Effect of F-doping in $ROFeAs$	17
2.9 Spin Density Wave	19
2.10 Superconductivity and Magnetism	20
3 Methodology	23
3.1 Introduction	23
3.2 Classical Green's Functions	23
3.3 Green Functions Formalism	24
3.3.1 Equation of Motion	25
3.3.2 Green Functions Formulation with reduced hamiltonian	27
3.3.3 For localized electrons	36
3.3.4 For Pure Superconducting System	40
4 Result and Discussion	42

List of Figures

2.1	The Meissner effect.	4
2.2	Phase diagram of type I and type II superconductors.	6
2.3	A picture of an attractive interaction (phonon interaction).	8
2.4	High-temperature superconducting materials discovered since 1986 and their critical temperature(T_c) under the maximum pressure	9
2.5	Tetragonal structure of $ROFeAs$	13
2.6	Temperature dependence of electrical resistivity of $LaFeAs$ ($O_{1-x}F_x$).	14
2.7	Spin density wave	20
2.8	Phase diagram with fluorine doping in $SmO_{1-x}F_xFeAs$	22
4.1	SSuperconducting order parameter vs. temperature for pure $SmO_{1-x}F_xFeAs$ superconductor.	43
4.2	Superconducting critical temperature vs. magnetic order parameter.	43
4.3	Antiferromagnetism transition temperature (T_m) vs magnetic order parameter(η).	44
4.4	the superconducting critical temperature and AFM transition temperature vs. magnetic order parameter.	44

Abstract

Superconductivity and magnetism were previously thought as incompatible until the discovery of some rare earth ternary compounds that show the coexistence of superconductivity and magnetism. In some of the recently discovered iron-based layered superconductors, superconductivity and magnetism coexist. In the present work we examine the possibility of coexistence of antiferromagnetism and superconductivity in samarium arsenide oxide superconductor ($SmAsO_{1-x}F_xFe$). Using a model of the Hamiltonian and retarded double time Greens function formalism, we found expressions for superconducting transition temperature (T_c), superconductivity order parameter ($\Delta_{sc}(T)$), AFM order parameter (η), and AFM transition temperature (T_m). We obtained the phase diagrams ($T_c v_s \eta$) and ($T_m v_s \eta$) to obtain the region where both orders ,i.e, superconductivity and AFM coexist. The region under the intersection of the two merged graphs shows that superconductivity and AFM coexist in the system($SmAsO_{1-x}F_xFe$).

Acknowledgements

I would like to express my sincere thanks to my advisor Prof. P. Singh for his Unlimited and constructive guidance, advice, suggestions ,comments His scientific excitement, integral view on research and overly enthusiasm, has made a deep impression on me. I would like to thank to all friends especially Ato Workeneh Abebe(M.sc in Economics) for providing encouragement and support during my work. I am grateful to all my families for their effort and encouraging me to do my work patiently especially my Father Mebrahtu Abreha. Above all I thank my Lord to his eternal love, kindness and support.

Chapter 1

Introduction

The history of superconductivity as a phenomenon is very rich, consisting many events and discoveries. Superconductivity is a phenomenon occurring in a certain materials at extremely low temperature, characterized by exactly zero electrical resistance. It was discovered in 1911 by Heike kamerlingh Onnes, who was studying the resistance of solid mercury at extremely low temperatures using the recently-discovered liquid helium as a refrigerant. At the temperature about 4.2K, he observed that the resistance abruptly disappeared [1].

Superconductivity has been found early in various elements such as mercury, lead, and aluminum. Most of the early superconductors are superconducting at extremely low transition temperature and low magnetic field. Some of the basic features of Sc were explained by Ginzburg and Landau, and Bardeen, cooper, and schriber, but the basic mechanism for understanding and solving problems in physics. superconductivity and magnetism would be antagonistic because of competitive nature (Meissner effect) and the internal field generated by magnetic ordering. , However, the discovery of a number of magnetic superconductors has allowed for better understanding as superconductor in ferropnictides. In this study we attempt to investigate theoretically coexistence of antiferromagnetism and superconductivity in ferromagnetic in a superconducting compound $\text{SmFeO}_{1-x}\text{F}_x\text{As}$.

Until 1986 the record for highest critical temperature was 23K for Nb_3Ge . In 1986 a

new La- Ba-based copper-oxide superconductor, $(La, Ba)_2CuO_4$, with critical temperature of 35K was discovered by Alex Müller and Georg Bednorz [2]. During the past decades it was subsequently established that superconductivity in all of these high temperature superconductors (HTS) containing Y, Bi, Tl, and Hg instead of La can be maintained up to much higher magnetic field and temperature. Moreover, materials of this class of oxides have been discovered with transition temperature well above 100K. In 2001, the discovery of non-oxide based superconductor in MgB_2 by Nagamatsu and Akimitsu [3] has restored the huge interest in the field of superconductivity. In February 2008, Hideo Hosono (from the Tokyo Institute of Technology in Japan) [4] has discovered an iron-based superconducting material in LaOFFeAs. The critical temperature for this iron-arsenide compound with lanthanum, oxygen and fluorine is 26K. Moreover, subsequent studies clarified that replacement of La by other rare earth elements increases the transition temperature markedly: 41K for Ce, 52K for Pr, 52K for Nd, and 55K for Sm. Superconductivity has also been discovered in fluorine-free systems, including $RFeAsO_{1-y}$

(R=La, Ce, Pr, Nd, Sm, Gd and Tc = 31K-55K), it was surprising that there could be another material other than the cuprate which could become superconducting at such elevated temperatures. The recent discovery of non-oxide superconductors in MgB_2 and iron-based compound ROFeAs would also assist theoretical physicists to be closer to a fundamental understanding in the basic mechanism behind high-temperature superconductivity.

Most of the physical properties of superconductors vary from material to material, such as the heat capacity, the critical temperature, critical current density, and critical field at which superconductivity is destroyed. The coexistence of superconductivity and magnetism has been an interesting topic in condensed matter physics. They are often thought to be incompatible. According to BCS theory a superconductor expels a magnetic field, which in turn destroys superconductivity. However, both superconductivity and magnetic ordering has been seen in harmony (coexists) in some of rare earth compound.

The coexistence of superconductivity and antiferromagnetism is quite peaceful and very weakly influences each other. From recent discovery of superconductivity in the rare-earth iron-based oxide system ($RO_{1-x}F_xFeAs$), it is generally believed that magnetism play fundamental role in superconducting mechanism like copper-oxide because superconductivity occurs when mobile electrons or holes are doped into AFM parent compound.

Experiment has been revealed that superconducting and magnetic phases are interplayed in samarium iron pnictide superconductor ($SmFeAs(O_{1-x}F_x)$) with the long range of ($0.1 \leq x \leq 0.15$). In this paper we studied theoretical coexist of superconductivity and Antiferromagnetism in $SmFeAs(O_{1-x}F_x)$. For this reason we include literature review on magnetism, superconductivity, and iron based superconductors in the second chapter, mathematical method and formulation of the problem in the third, in the fourth chapter we include results and discussion and in the final chapter we put some important conclusions of the study.

Chapter 2

Literature Review

2.1 Meissner effect

The Meissner effect was discovered in 1933 by Water Meissner and Robert Ochenfield [5]. It is one of the properties of superconducting materials. When a superconductor below T_c is placed under a weak external magnetic field B , it repels the magnetic flux (field) B completely from its interior. It does this by setting up electric currents near its surface. It is the magnetic field of these surface currents that cancels out the applied magnetic field within the bulk of the superconductor. Near this surface, within a distance called the London penetration depth, the magnetic field is not completely canceled. This exclusion of magnetic flux from superconductor ($B=0$) is known as Meissner effect.

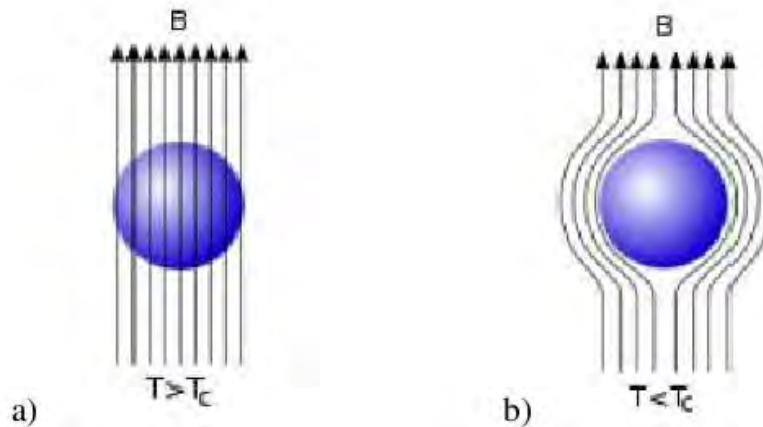


Figure 2.1: The Meissner effect.

- a) Magnetic field penetrating a superconductor above critical temperature.
- b) Magnetic field expelled from it below the critical temperature.

2.2 Types of superconductors

The superconducting state in specimen is destroyed if the specimen is placed in a sufficiently strong magnetic field (critical field, B_c) or if we generate strong enough currents (critical current $> 105A/cm^2$). Based on this we distinguish two types of superconductors: type I and type II. Type I super-conductor expels a magnetic field for $B < B_c$ while for $B > B_c$ superconductivity is destroyed and the field penetrates completely into the sample. A type II superconductor expels field in the normal state completely under B_{c1} . Most pure elemental superconductors, except niobium, technetium, and vanadium are type I and Almost all impure and compound superconductors are Type II superconductors. When B exceeds B_{c1} the field is only partially excluded, and the bulk specimen remains to be superconducting. Between B_{c1} and B_{c2} the superconducting state coexists with normal state regions where magnetic field penetrates into the sample. The Field uniformly penetrates the specimen in form of vortices. This mixed state is called vortex state.

Vortex state describes swirling tubes of electrical current induced by an external magnetic field which penetrates into the surface of a superconducting material. Inside the vortices the specimen is in the normal state surrounded by the superconducting state. Above field B_{c2} the flux penetrates completely and superconductivity vanishes.

An important difference in type I and type II superconductor is in the mean free path of the conducting electrons in the normal state. If the coherence length ζ is longer than the penetration depth λ , the superconductor will be type I. When the mean free path is short, then the ζ is also short and the λ is large, so the superconductor will be type II.

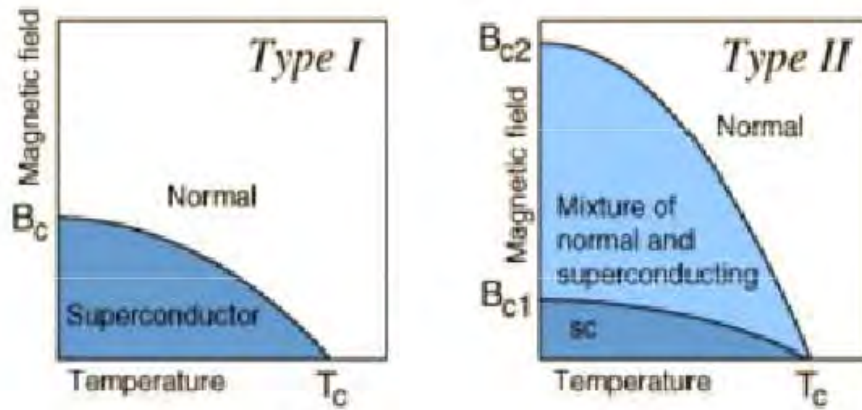


Figure 2.2: Phase diagram of type I and type II superconductors.

2.3 Phenomenological and BCS theory

The theory of superconductivity has developed along two lines; the phenomenological and microscopic theory. The phenomenological treatment was initiated by F.London [7] who modified the Maxwell electromagnetic equation so as to allow for the Meissner effect. His theory explained the existence and order of magnitude the penetration depth. The treatment was extended by VL Ginzburg and LD Landau and by AB Peppereid who in particular emphasized the concept of coherence length (ζ). AA Abrikosov used these ideas to develop a model for alloy for superconductors. He showed that if the electronic structure of the superconductor were such that the coherence length becomes smaller than the penetration depth, one would get magnetic behavior similar to type II of superconductors, with two critical fields B_{c1} and B_{c2} .

The microscopic theory of superconductivity was initiated by H.Frohlich [8], who was first recognizing the importance of the interactions of electrons with lattice. Discovery of the isotope effect on T_c supported his assertion that the electron-phonon interaction plays an essential role in superconductivity. The detailed microscopic theory was developed by John Barden, Leon cooper and John Schrieffer in 1957 [9]. Their theories of superconductivity became known as the BCS theory. In the BCS theory framework, superconductivity

is microscopic effect which result from condensation of electron pair called cooper pair.

A cooper pair is the name given to the electrons that are bound together in a certain manner and first discovered by Leon Cooper. Cooper showed such binding will occur in the presence of an attractive potential, no matter how weak. In the BCS theory, a system of electrons is interacting with phonon which is the quantized vibration of the lattice. There is a screened coulomb repulsion between pairs of electrons, but in addition there is also attraction between them via the electron-phonon interaction. If the net effect of these two interactions is attractive, then the lowest energy state of the electron system has a strong correlation between pairs of electrons with equal and opposite momenta and opposite spin.

A simplified explanation of cooper pair formation: an electron moving through the conductor will attract the positive ions in the lattice. This attraction can distort the positively charged ions in such away as to attract other electrons (the electron-phonon interaction). The attraction due to the displace ion can overcome the electron repulsion due to the electrons having the same charge and cause them to pair.

BCS theory explored superconductivity at a temperature close to zero for elements and simple alloys (conventional) superconductors. However, at high temperature and with different superconductor system, the BCS theory has subsequently become inadequate to fully explain how superconductivity is occurring.

2.4 High Temperature Superconductivity and its Mechanism

After the discovery of superconducting mercury by Kamerlingh Onnes in 1911, the search for new superconducting materials lead to a slow increase in the highest known transition temperature(T_c) over the decades reaching a plateau at 23K with the discovery of superconducting of Nb_3Ge by Gavalier in 1973. After 13 more years, higher transition

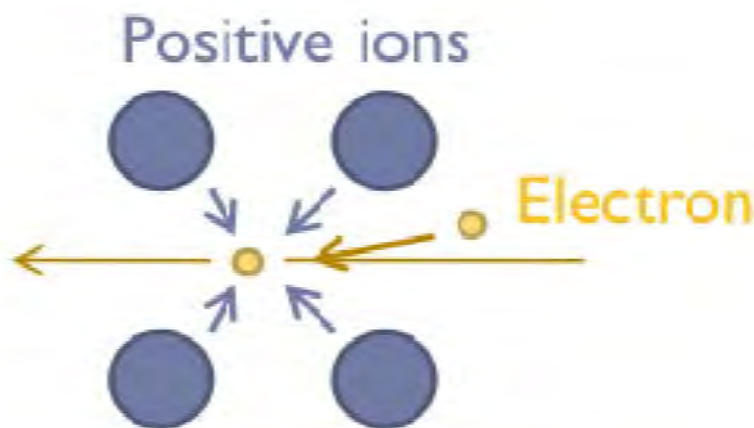


Figure 2.3: A picture of an attractive interaction (phonon interaction).

temperature was discovered in 1986 in LBCO (a mixed oxide of lanthanum, barium, and copper) by Bendnorz and Muller, for which they were awarded the Nobel prize in 1987. The term high temperature superconductor was first used to designate for this newly discovered cuprate oxide. Another big jump to T_c about 90K followed quickly, with the discovery of 123 class of materials, exemplified by $YBa_2Cu_3O_7$ ($YBCO$), the Y (yttrium) can be replaced by many other rare earth elements example La, Nd, Sm and Gd with similarly high T_c . Shortly thereafter, still higher T_c values were found in the BSCCO (mixed oxide of bismuth, strontium, calcium and copper) and the TBCCO system (mixed oxides of thallium, barium calcium, and copper). In all of these systems, copper oxide planes form a common structural element, which is thought to dominate the superconducting property [10].

In the context of superconductivity, high superconductivity (high- T_c or HTS) are material that have a superconductivity transition temperature above the temperature historically been taken as the upper limit allowed by BCS theory. This is above the 1973 record of 23K that had lasted until copper- oxide materials were discovered [11].

Recently, iron- based superconductors with the critical temperature as high as 55K

have been discovered. These are often also referred to as high-temperature superconductors. High- T_c superconductors (unconventional superconductors) differ in many important ways from conventional superconductors, such as mercury or lead, which are adequately explained by BCS theory.

All known high- T_c superconductors are type II superconductors which allow magnetic fields to penetrate their interior in quantized units of flux, meaning that much higher magnetic fields are required to suppress superconductivity. If we call, without strict definition, the superconducting materials with T_c exceeding the record value of 23K before 1986 as high temperature superconductors (HTS), its now high-temperature realized in eight families of materials. Starting from the cuprates (1986), they are $Ba_{1-x}K_xBiO_3$ (1988), intercalated C_{60} (1991), borocarbide (1994), HfNCI (1998), MgB_2 (2001), Ca under high-pressure (2006), and the newly discovered Fe pnictides (2008) [12].

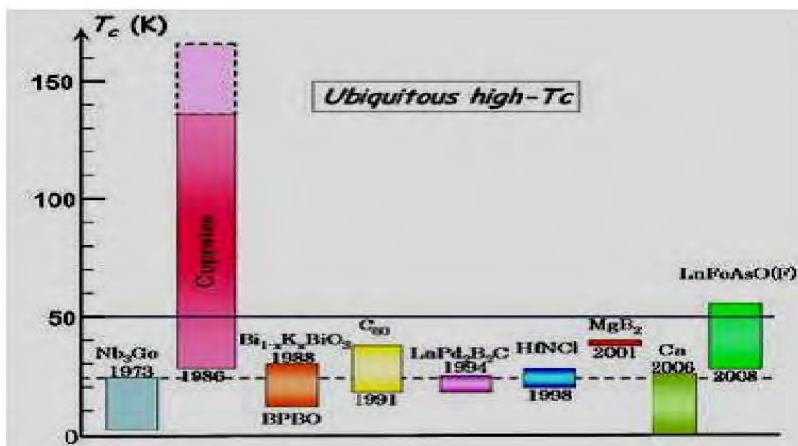


Figure 2.4: High-temperature superconducting materials discovered since 1986 and their critical temperature(T_c) under the maximum pressure

The mechanism of superconductivity is one of the most exciting areas in the study of high- T_c superconductors. Understanding the mechanism superconductivity will clarify how magnitude of T_c can reach and how it may be pushed higher, as well as why its pressure dependence is so large [8].

The mechanism that causes the electrons to form pairs in high- The high temperature

superconductors is not clearly known. However, lattice vibrations alone are not strong enough to maintain electron pairing at elevated temperatures. Pairing mechanisms of magnetic origin have been proposed, mainly to justify the high critical temperatures of HTS: the magnetic exchange energies are about four times the phonon energies. In this case, the electron pairing would have a wave function with d-wave symmetry. One of the most dominant theories that contain d-wave symmetry is the spin wave model. According to this theory, the carrier leaves a magnetic disturbance (a spin wave) in its wake. This wake pulls a second carrier, so that the two forms a Cooper pair. The spin waves are short lived, so they are often called spin fluctuations [13].

Thus, determining whether the pairing wave function has d-wave symmetry is essential to test the spin fluctuation mechanism. In addition to d-wave symmetry the pairing symmetry can be an extended s- wave, p- wave might be result of the spin fluctuation mechanism. Pairing symmetry provides clues to the identity of the superconducting pairing mechanism which is essential for the development of the theory of high temperature superconductivity. In general possible orbital pairing states include s-wave, an extended s-wave, p-wave and d- wave states. In the s-wave state, the energy gap (k) is isotropic; i.e., (k) is constant over the Fermi surface.

2.5 Superconductivity and Magnetism in Fe-pnictide Superconductors

The recently discovered quaternary arsenide oxide superconductor $La(O_{1-x}F_x)FeAs$ with the superconducting critical transition temperature (T_c) of 26K, has been quickly expanded to another family of high- T_c superconducting systems besides copper oxides by the replacement of La with other rare earth elements. One of the superconductors that obtained replacing La by Sm is samarium-arsenide oxides $Sm(O_{1-x}F_x)FeAs$ with a critical temperature T_c of 55K, which is the highest among all materials besides copper oxides up

to now [14]. A superconductivity in Neodymium arsenide oxides $Nd(O_{1-x}F_x)FeAs$, with the onset resistivity transition at 51.9K and Meissner transition at 51K was synthesized by replacement of La with Nd which is also non-cu prate compound that superconductors above 50K. The other discovered bulk superconductivity is in the praseodymium arsenide oxides $Pr(O_{1-x}F_x)FeAs$ with an onset drop of resistivity as high as 52K is also obtained by substitution of La by Pr. Replacement of La by Ce, leads to a large increase in critical temperature (T_c) from 26K to 41K in layered $CeO_{1-x}F_xFeAs$. The superconductivity has been also discovered in oxygen free AFe_2As_2 (A=Ba, Sr, Ca) [15]. Like the cuprates, the pnictides are highly two dimensional, their parent material shows AFM order below 150K, and superconductivity occurs upon doping of either electrons or holes into the FeAs layers. There is a growing consensus among researchers that Mott physics does not play a significant role for the iron pnictides, which remain itinerant for all doping levels. relatively small value of the observed magnetic moment per Fe atom [15], cause the spin density wave which is a type of Antiferromagnetic is associated with structural phase transition from tetragonal to orthorhombic. Cruz et al. Neutron-scattering experiments reveal that a structural phase transition in LaFeAsO is at T_M 155K where T_s is structural transition temperature. This result demonstrates that LaFeAsO undergoes an abrupt structural distortion below 155K, and the symmetry changes from tetragonal (space group P4=nm) to orthorhombic (space group Cmma) at low temperatures. Furthermore, they carried out order parameter measurements to determine whether or not the ordered magnetic scattering at low temperatures in LaFeAsO is indeed associated with structural-phase transition. And they found the ordered magnetic moment vanishes at temperature 137K, approximately 18K lower than the temperature at which the structural phase transition occurs. Therefore, the magnetic anomaly at approximately 150K is caused by structural distortion. In contrast, neither structural nor magnetic anomaly was observed in superconducting state [18].The La-NMR experiment result has also shown that the magnetic ordering is related to the structural distortion. The structural phase

transition have seen in other pnictides such as SmOFeAs, CeOFeAs and so on with different Ts. Experiments and theoretical calculations suggest that ROFeAs exhibits a AFM instability that is suppressed by doping with electrons to induce superconductivity.

2.6 Crystal Structure of Fe-pnictide Superconductors

The layered iron superconductors, discovered by Kamihara and co-workers [17], now comprise a rather large family of materials, with four distinct crystallographic types. The first one is RFeAsO (R=rare earth element) which is called the 1111 structure (space group P4=nmn). Figure 2.4 below shows the first type of crystal structure. The RO and FeAs layers are stacked along the c-axis. The first discovered iron-pnictide superconductor $LaFeAs(O_{1-x}F_x)$ has this structure, and various rare-earth elements such as Sm, Ce, Pr, and Nd can enter the R site [18]. The Fe atoms form a planar square lattice which is sandwiched by As square lattice or two-dimensional network of $FeAs_4$ tetrahedra is formed. The FeAs layer is a conduction plane for charge carriers and a main stage of superconductivity. The other building block $RO_{1-x}F_x$ is a charge reservoir layer, controlling the carrier density or chemical potential [12]. The unit cell contains two molecules, and the chemical formula is represented by $(La_2O_2)(Fe_2 - As_2)$. The Fe_2As_2 layer, which is sandwiched between the La_2O_2 layers, serves as a carrier conduction path. Thus, conduction carriers are two-dimensionally confined in the Fe_2As_2 layer, causing strong interactions among the electrons. All iron-pnictide superconductors- are layer with tetragonal structure at room temperature.

The second iron-pnictide family is abbreviated as 122, and is well-known in heavy-fermions (HF) compounds. The third structure was reported in superconducting LiFeAs, called the 111 structure. LiFeAs crystallizes into the Cu_2Sb -type tetragonal structure containing the FeAs layer with an average iron valence of +2 like those for the 1111 or 122

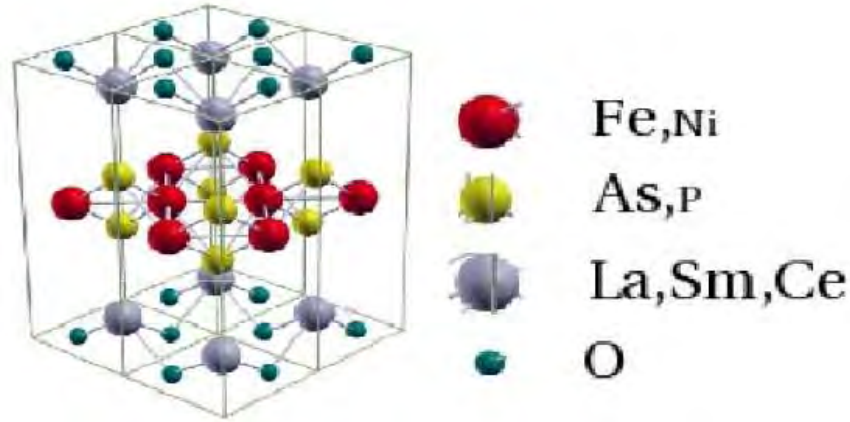


Figure 2.5: Tetragonal structure of ROFeAs.

parent compound. Recently, superconductivity has been reported at 8K in FeSe compounds with the PbO -type structure. This structure, shortened as the 111 structure [18].

2.7 Physical Properties $\text{R}(\text{O}_{1-x}\text{F}_x)\text{FeAs}$

The superconductivity in the high T_c cuprate arises from either electron or hole doping in the non superconducting parent compounds. The parent material shows anomalies such as in resistivity. Owing to this, some researchers share the view that in so far as the normal state properties reflect the electronic structure that underlies high T_c superconductivity, it is necessary to develop an understanding of the normal state before the superconducting state can be understood.

Superconductivity in the newly discovered rare-earth iron-based oxide systems ROFeAs (R=La, Ce, Nd, Pr and Sm) also arises from either electron or hole doping of their non- superconducting parent compounds. The parent material LaOFeAs is metallic but shows anomalies near 150K in both resistivity and D.c. magnetic susceptibility [22]. Dong et al. investigated the systematic F-content dependence of the electrical resistivity of $\text{LaFeAs}(\text{O}_{1-x}\text{F}_x)$, which is shown in Fig below. The resistivity of undoped LaFeAsO

shows weak temperature dependence with a high value at high temperatures, and exhibits a steep drop at approximately 150K with an upturn below 50K. The resistivity of the 2 F-doped sample decreases and the 150K anomaly shifts to a lower temperature and becomes less pronounced. In the 3 F-doped sample, no anomaly was observed and a superconducting transition occurs at 17K. With further F doping, superconducting-transition temperature increases and leads to the highest $T \approx 28K$ for 10 F doping [18]. The measurements in $LaFeAs(O_{1-x}F_x)$ by Kohama et al. [23] and Klingeler et al. [24]

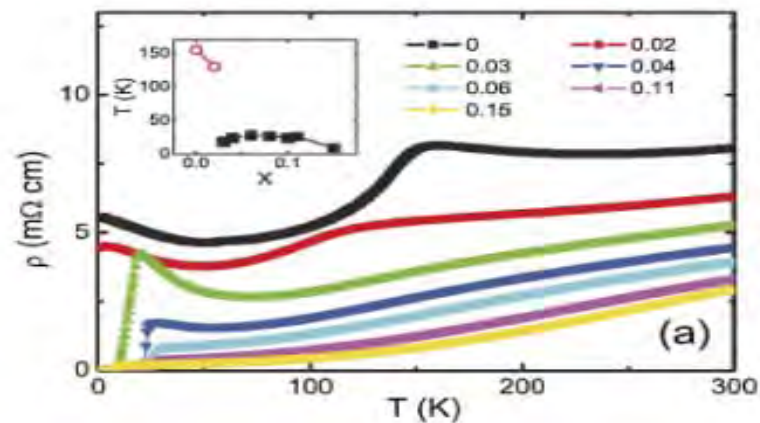


Figure 2.6: Temperature dependence of electrical resistivity of $LaFeAs(O_{1-x}F_x)$.

was revealed that the x_{bulk} of $LaFeAs(O_{1-x}F_x)$ is independent of local-moment effects by rare- earth elements, and is affected only by the iron 3d electrons. In both reports, the x_{bulk} of $LaFeAsO$ shows a gradual decrease from room temperature and exhibits a small drop at T_S where the structural transition occurs. Below approximately 50K, x_{bulk} shows an upturn behavior, which would be described to an impurity contribution. The temperature dependences of the x_{bulk} of the F-doped compounds are different between the above two reports. The bulk of the F-doped sample reported by Kohama et al. shows an increasing behavior with decreasing temperature, but that reported by Klingeler et al. shows a gradual decrease with decreasing temperature as in the undoped $LaFeAsO$. The zero resistivity and the large diamagnetic susceptibility show that $LaOFeAs$ becomes a superconductor by F-doping [4].

The resistivity increases slightly with decreasing temperature, but below roughly 145K, the resistivity drops steeply. After F doping, the overall resistivity decreases and the 145K anomaly shifts to lower temperature and becomes less pronounced. At higher F doping, the anomaly disappears and a superconducting transition occurs. The resistivity behavior of the pure CeOFeAs is very similar to that of LaOFeAs, except that a resistivity up turn was observed in the later compound at low temperature. As we saw earlier, the anomaly at 150K is caused by spin- density-wave instability. As Sm has a smaller covalent radius comparing with La, Ce, Pr and Nd, the inner chemical pressure that caused by the shrinkage of crystal lattice is thought to be an important factor that enhances T_c , as proposed in a theoretical calculation, where it is indicated that the T_c may be enhanced by the increase of dopping integral, which can be achieved by the shrinkage of the lattice.

The excitement with this discovery was largely stimulated with some close similarities between iron-based SC and HTSC:

- 1) Both systems are layered in structure.
- 2) Parent compounds are antiferromagnets and superconductivity appears upon doping which exceeds critical value. At the same time antiferro- magnetic phase is suppressed.
- 3) The phase diagrams are similar.
- 4) Both are type II superconductors.

2.8 Mechanism of superconductivity in Fe-pnictide

In the Bardeen-Cooper-Schrieffer theory of superconductivity, electrons form Cooper pairs through an interaction mediated by vibrations of the crystal(phonons). Like lattice vibrations, magnetic fluctuations can also produce an attractive interaction creating Cooper pairs, though with spin and angular momentum properties different from those of conventional superconductors [25].

The newly discovered iron-pnictid superconductor is unconventional superconductivity such as that in copper oxides. The reasons why unconventional pairing may be realized in iron pnictides: (i) T_c is very high, compared with conventional phonon-mediated BCS superconductors (ii) electron-phonon coupling is expected to be weak according to first-principles calculations [21].

Up to now, many theoretical studies of the iron-pnictid superconductors have been reported. As for the superconducting pairing state, most of them have proposed the s pairing state. Here, we introduce some of the works suggesting the s pairing state, which were reported just after the discovery of the superconductors. A.V.Chubukov et al. suggest that both magnetic and pairing instabilities are determined by the same inter band pair doping which transforms two fermions near the hole Fermi surface (FS) into two fermions near the electron Fermi surface (and vice versa). When electron and hole pockets are nearly identical, spin density wave(SDW) instability occurs at a higher T. When the near identity is broken by either hole or electron doping, the Cooper instability comes first. This pairing interaction sets the gaps in hole and electron pockets to be of equal magnitude Δ , but of opposite signs (an extended s-wave symmetry, s+) [15].

Ding et al. have performed ARPES measurements on the Superconducting iron pnictide and two superconducting gap without node were observed on small hole-like and electron-like Fermi surface sheets. They suggest that the pairing mechanism originates from the inter-band interactions between these two nested Fermi-surface sheets. Similar experimental results from different groups on the 1111 system have been reported and they strongly suggest that a) the superconducting gap is nodeless, which excludes the p-wave and d-wave pairing states with nodes of the gap on the Fermi surfaces but consistent with s wave pairing, and that b) the magnitude of superconducting gap is orbital-dependent. Node less superconducting gap was also suggested from magnetic penetration-depth measurements. Hashimoto et al. Magnetic penetration-depth measurements on under doped single crystals of $PrFeAsO_{1-\delta}$ ($T_c = 35$ K), suggests a nodeless superconducting gap. A

similar two-nodeless gap model is also applied in $SmFeAsO_{1-x}Fx$ ($T_c = 45$ K), but the result suggesting a single fully gapped order parameter with a small anisotropy reported in single crystals of $NdFeAsO_{1-x}Fx$ ($x = 0.1$).

Mazin et al. argued that superconductivity realized in the iron-pnictide compounds is unconventional and mediated by antiferromagnetic spin fluctuations. Its pairing state is an extended s-wave pairing with a sign reversal of the order parameter between different Fermi surface sheets [26].

They claimed that doped LaFeAsO represents the first example of multi gap superconductivity with a discontinuous sign change in order parameter between the bands. Their scenario is based on the calculated Fermi surfaces for the undoped LaFeAsO, and the superconductivity is induced by the nesting-related antiferromagnetic spin fluctuations near the wave vectors connecting the electron and hole pockets.

Kuroki et al [27] constructed a minimal model, where all the necessary five d-bands are included and calculated spin susceptibility and charge susceptibility within random phase approximation. Furthermore, they investigated superconducting properties using the linearized Eliashberg equation, and concluded that the multiple spin-fluctuation modes arising from the nesting across the disconnected Fermi surfaces realize an extended s-wave pairing, in which the gap changes sign between the hole and electron Fermi surfaces across the nesting vector. This unconventional s-wave pairing is the same as the s state proposed by Mazin et al.. Kuroki et al. To identify the mechanism of iron-pnictide superconductivity, the determination of the presence or absence of nodes in the superconducting gap is quite important.

2.8.1 Effect of F-doping in RFeAs

To achieve superconductivity, two methods are commonly used, doping and applying pressure. Either electron doping or hole doping can introduce superconductivity. In the cuprates doping is necessary for introducing mobile charge carriers, since the parent

compounds are Mott-Hubbard insulators. Superconductivity in the newly discovered rare-earth iron-based oxide systems ROFeAs (R is rare-earth metal) also arises from either electron or hole doping of their non-superconducting parent compounds. Since the parent material ROFeAs is metallic, and doping does not appear to change the charge density very much. F-ion substitution for the O sites changed the bond length and bond angle in the distorted LaO tetrahedron, whereas weaker geometric effects were observed in the FeAs layer. Further, the F-doping induced large decreases in the c-axis length and the La-As distance, suggesting an enhancement of the polarizations in the $(LaO)^{\delta+}$ and $(FeAs)^{\delta-}$ layers as a result of electron transfer between two layers. The enhanced polarization and Fe-Fe interaction in the FeAs layer are likely to suppress the transition leading to the emergence of superconducting phase.

In general, the effect of F-doping at the O sites are summarized as follows : a) the F-doping acts as an electron donor, leading to a supply of the extra electrons to the FeAs layer, which results in a shift of the chemical potential to lower binding energy side. b) the c-axis length and La-As distance are shortened as result of the enhancement of the charge polarization of the $(LaO)^{\delta+}$ and $(FeAs)^{\delta-}$ layers. C) the Fe-Fe distance decreases, which may enhance the interaction among 3d electrons. d) the distortion of the La_4O tetrahedron is relaxed largely, whereas less structural changes take place in the FeAs tetrahedron. It is likely that interplay of these effects may prohibit the crystallographic and magnetic transitions to occur and generate the superconducting phase [28].

The effects of F-doping observed in $LaO_{1-x}FxFeAs$ are also observed in other rare earth compound. Experimental measurement shows that the F doping iron pnictide have smaller lattice parameter as compared to the parent compound. For example, the lattice parameter for the parent CeOFeAs and $CeO_{1-x}FxFeAs$ $x=0.16$ of F doping compound obtained this is similar to other rare earth substitutions, and indicates the covalent character of the intra-layer chemical bonding due to the smaller covalent radius of fluorine than oxygen.

2.9 Spin Density Wave

Spin-density wave (SDW) occurs at low temperature in anisotropic, low-dimensional materials or in metals that have high densities of states at the Fermi level $N(E_F)$. Other low-temperature ground states that occur in such materials are superconductivity, ferromagnetism and antiferromagnetism. Experimental investigations show that the SDW is a kind of antiferromagnetic state, with the electronic spin density forming a static wave. The density varies periodically as a function of position with no net magnetization in the entire volume. The SDW transition occurs when the spatial spin density modulation is due to delocalized or itinerant electrons rather than localized ones. In normal state the density of electrons spins polarized upward canceled by density of downward polarized spins[8].

SDW ground state is obtained from the single band Hubbard model with in the Hartree-Fock approximation and assuming that the nesting of the Fermi surface exists only in certain direction of the Fermi surface. The direction of the Fermi surface where nesting exists will be instable with respect to the AFM formation whereas the superconductivity instability may occur in the rest of the part of the Fermi surface, provided there exists some attractive interaction between the quasi particles mediated by some boson exchange. Therefore, one can present a model to study the coexistence of superconductivity and AFM, that incorporates two competing physical processes involving electron-hole AFM like pairing of opposite spins with a net momentum difference (Q) between the conjugates and electron-electron (superconducting) pairing of opposite spins with total momentum zero.



Figure 2.7: Spin density wave

2.10 Superconductivity and Magnetism

The interplay of magnetism and superconductivity is a fundamental problem in condensed matter physics. These two phenomena were thought mutually antagonistic. In conventional superconductors (BCS theory of superconductivity), local magnetic moments break up the spin-singlet Cooper pairs and hence strongly suppress superconductivity, an effect known as pair-breaking. Typically, magnetic fields destroy superconductivity because the energy they generate perturbs the close interaction between pairs of electrons that is a prerequisite for superconductivity. The most common way that a magnetic field destroys superconductivity is by disturbing the orbital effect, where the electrons in a pair orbit each other, acquiring more and more energy from the magnetic field. Once this energy becomes greater than that which unites the two electrons, the electron pairs break apart and superconductivity is suppressed. The other way magnetic fields can destroy superconductivity is when two electrons have what is called opposite spin; this is when in addition to the two electrons orbiting one another, they also are spinning like tops but in opposite directions, called s-wave spin. When the magnetic field is turned on, one electron gains energy while the other loses. "If the difference is bigger than the amount of energy holding the electrons together, then they fly apart and superconductivity has gone," explained

Naughton [29].

However, in a limited class of inter-metallic systems, superconductivity occurs even though magnetic ions with a local moment occupy all of one specific crystallographic site, which is well isolated and de-coupled from the conduction path. The possible coexistence of superconductivity with various types of magnetism carried by localized magnetic moments and itinerant electrons is critically discussed in connection with several existing materials such as rare earth ternary compounds [$(RE)Mo_6S_8$, (RE=Gd,Tb,Dy and Er) $(RE)Mo_6S_8$ and $(RE)Rh_4B_4$], (RE=Nd ,Sm and Tm magnetic system[30], and has been recently revitalized by the discovery of the RNi_2B_2C (R=Y,Tm,Ho) system. In all three systems, both SC and antiferromagnetic (AFM) ordered states coexist. The coexistence of superconductivity and ferro-magnetism in the same compound has been put forward theoretically by V. Ginzburg in 1957 [31].

In his theoretical explanation, the coexistence of magnetism and superconductivity occurs when ferromagnetic field is smaller than the thermodynamic critical field of superconductor. The coexistence of superconductivity and antiferromagnetism is quite peaceful and very weakly influences each other, because the antiferromagnetic molecular field is effectively averaged out within the scale of the superconducting coherence length. Superconductivity coexisting with ferromagnetic order was recently observed in UGe_2 and URhGe. This superconducting phase is found within the ferromagnetic phase and disappears in the paramagnetic region. The coexisting superconductivity with ferromagnetic is strongly suggesting that the pairing mechanism is magnetic in origin [32].

Experimental study on the newly discovered iron pnictide superconductor found that magnetism and superconductivity coexists in the long rang doping in $SmO_{1-x}F_xFeAs$ ($0.1 \leq x \leq 0.15$)[33].

Recently, Muon Spin Relaxation measurement revealed that superconducting and magnetic phases coexists in $LaFeAs(O_{1-x}F_x)$ with $x = 0.06$ ($T_c = 18K$) [34].

These two phases indeed coexist in the form of macroscopic phase separation, and

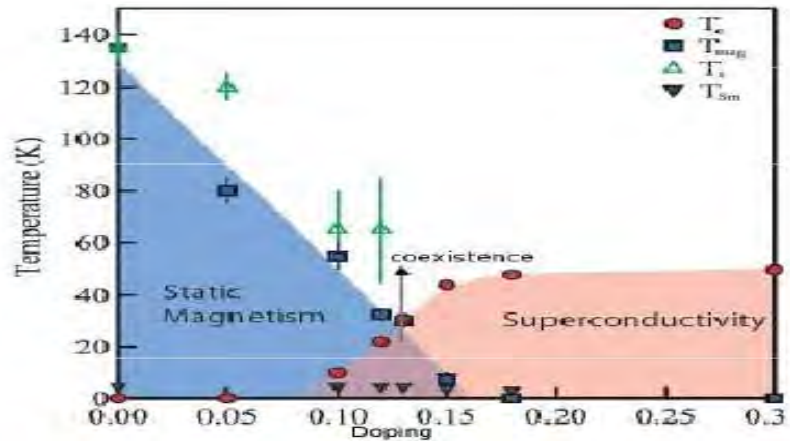


Figure 2.8: Phase diagram with fluorine doping in $SmO_{1-x}F_xFeAs$

more interestingly, that a spin glass-like magnetic phase develops in conjunction with superconductivity in the paramagnetic phase[19]. This accordance strongly suggests a common origin of the electronic correlation leading to these two competing phases.

Chapter 3

Methodology

3.1 Introduction

In this study we have used a quantum field theory (mean-field theory) by using a Green functions techniques to obtain the expression for superconducting transition temperature T_c and order parameters (Δ, η) . The Green's functions are useful, because they are flexible enough to describe the effects of retarded interaction and all the qauntities of physical interests can be derived from them.

3.2 Classical Green's Functions

The Green's function method is a very useful method in the theory of ordinary and partial differential equations. It has a long history with numerous applications. Poisson's equation with electrical potential, ϕ and a fixed charge distribution, ρ is

$$\nabla^2 \phi_{(r)} = -\frac{1}{\epsilon_0} \rho_{(r)} \quad (3.2.1)$$

It turns out to be a good idea instead to look for the solution G of a related but simpler differential equation

$$\nabla_r^2 G_{(r)} = \delta_{(r)} \quad (3.2.2)$$

where $\delta_{(r)}$ is the Dirac delta function. $G_{(r)}$ is called the Green's function for the Laplace operator, ∇_r^2 . The electrical is given as

$$\phi(r) = -\frac{1}{\epsilon_0} \int dr' G_{(r-r')} \rho(r')$$

The easiest way to find $G_{(r)}$ is by Fourier transformation, which immediately gives

$$-k^2 G_{(k)} = 1 \implies G_{(k)} = -\frac{1}{k^2} \quad (3.2.3)$$

and hence

$$G_{(r)} = \int \frac{dk}{(2\pi)^3} e^{ik \cdot r} G_{(k)} = - \int \frac{dk}{(2\pi)^3} \frac{e^{ik \cdot r}}{k^2} = -\frac{1}{4\pi r}$$

3.3 Green Functions Formalism

Green functions or suitable modification of these functions have been applied in quantum field theory (mean-field theory) to statistical problems. The Green functions are essentially useful for summing over the restricted classes of perturbation theory diagrams and are very powerful when combined with spectral representations. In quantum field theory Green functions are known as propagator. This name is based on the idea that, in order to find the important physical properties of a system, it is essential to know, not the detailed behavior of each particle in the system, but rather just the average behavior of one or two typical particles. The quantities that describe this average behaviors are known as the one-particle and two-particle propagators.

Green function play the most important part in the field-theoretical treatment of the many-body problem. In our discussion we used only the retarded double-time Green function. It is defined as

$$G_{(t,t')} = \langle\langle \hat{A}_{(t)}; \hat{B}_{(t')} \rangle\rangle \quad (3.3.1)$$

$$G_{(t,t')} = -i\theta_{(t,t')} \langle\langle [\hat{A}_{(t)}, \hat{B}_{(t')}] \rangle\rangle \quad (3.3.2)$$

Where

$\langle\langle \dots \rangle\rangle$ is the abbreviated notation for the Green function,

$\langle \dots \rangle$ denotes the thermal average,

$\theta_{(t,t')}$ is the step function and

$\hat{A}_{(t)}, \hat{B}_{(t')}$ are operators in the Heisenberg representation, which can be expressed as the product of the quantized field operator. and let us consider $t' = 0$

$$\text{Then, } A_{(t)} = e^{(iHt)} A_{(0)} e^{(-iHt)}$$

Also A and B follows commutator or anticommutator relation. That is

$$[A, B] = AB - BA = 0 \text{ commutator operators and}$$

$$[A, B] = AB - BA \neq 0 \text{ anticommutator operators (non commutator operators).}$$

3.3.1 Equation of Motion

To obtain the equation of motion of the Green functions we differentiate eq(3.3.2) with respect to time t as

$$\frac{id}{dt} G_{(t,0)} = \delta_{(t,0)} \langle\langle [\hat{A}_{(t)}; \hat{B}_{(0)}] \rangle\rangle - i\theta_{(t,0)} \langle\langle \left[\frac{d}{dt} \hat{A}_{(t)}; \hat{B}_{(0)} \right] \rangle\rangle \quad (3.3.3)$$

$$i\hbar \frac{d}{dt} \hat{A}_{(t)} = [\hat{A}_{(t)}, \hat{H}]$$

If $\hbar = 1$

$$\frac{id}{dt} G_{(t,0)} = \delta_{(t,0)} \langle\langle [\hat{A}_{(t)}; \hat{B}_{(0)}] \rangle\rangle + \langle\langle [\hat{A}_{(t)}, \hat{H}]; \hat{B}_{(0)} \rangle\rangle \quad (3.3.4)$$

$\hat{A}_{(t)}$ and \hat{H} satisfy the following condition,

$$[\hat{A}_{(t)}, \hat{H}] = \hat{A}_{(t)}\hat{H} - \hat{H}\hat{A}_{(t)}$$

Then, equation of motion becomes;

$$\frac{id}{dt}G_{(t-0)} = \delta_{(t-0)} \langle [\hat{A}_{(t)}; \hat{B}_{(0)}] \rangle + \langle \langle \hat{A}_{(t)}\hat{H} - \hat{H}\hat{A}_{(t)}, \hat{B}_{(0)} \rangle \rangle \quad (3.3.5)$$

To solve this equation it is convenient to work with Fourier transform of this equation. A careful analysis show that the function depends on t and t' through $(t-t')$. Thus we can write

$$G_{(t,t')} = G_{(t,0)}$$

Let $G_{(\omega)}$ be the Fourier transform of $G_{(t-0)}$ such that

$$G_{(t-0)} = \int_{-\infty}^{\infty} G_{(\omega)} \exp(-i\omega(t-0)) d\omega \quad (3.3.6)$$

$$G_{(\omega)} = \int_{-\infty}^{\infty} G_{(t-0)} \exp(i\omega(t-0)) d(t-0) \quad (3.3.7)$$

and δ the Dirac delta function can be defined as

$$\delta_{(t-0)} = \int_{-\infty}^{\infty} \exp(-i\omega(t-0)) d\omega \quad (3.3.8)$$

Therefore eq(3.3.4) becomes

$$\omega G_{(\omega)} = \langle [\hat{A}_{(t)}, \hat{B}_{(0)}] \rangle + \langle \langle [\hat{A}_{(t)}, \hat{H}]; \hat{B}_{(0)} \rangle \rangle \quad (3.3.9)$$

Then $\omega G_{(\omega)}$ can be written as

$$\omega \langle \langle A, B \rangle \rangle = \langle [A, B] \rangle + \langle \langle [A, H], B \rangle \rangle \quad (3.3.10)$$

$$\omega \langle \langle A, B \rangle \rangle = \langle [A, B] \rangle + \langle \langle AH - HA, B \rangle \rangle \quad (3.3.11)$$

Since $\langle\langle A, B \rangle\rangle$ denote the Fourier transform of the Green functions involving the operator A and B.

3.3.2 Green Functions Formulation with reduced hamiltonian

To solve the properties of superconductivity we can use the following type Hamiltonian (or reduced Hamiltonian), which is given bellow.

$$H = \sum_{k\sigma} \epsilon_k a_{k\sigma}^\dagger a_{k\sigma} - V_{BCS} \sum_{k,k'} a_{k\uparrow}^\dagger a_{-k\downarrow}^\dagger a_{k'\downarrow} a_{-k'\uparrow} + \sum_{k,k',l,l'} \alpha_{kq} a_{k\uparrow}^\dagger a_{-k\downarrow}^\dagger b_l b_{l'} + h.c \quad (3.3.12)$$

We also use the equation of motion of Fourier transform, which is

$$\omega G(\omega) = \langle[A, B]\rangle + \langle\langle[A, H]; B\rangle\rangle \quad (3.3.13)$$

and we can take

$$G(t) = \langle\langle a_{k\uparrow}, a_{k'\uparrow}^\dagger \rangle\rangle \quad (3.3.14)$$

Then, the equation of motion in Fourier transform becomes

$$\omega G(\omega) = \langle[a_{k\uparrow}, a_{k'\uparrow}^\dagger]\rangle + \langle\langle[a_{k\uparrow}, H]; a_{k'\uparrow}^\dagger\rangle\rangle \quad (3.3.15)$$

First let us do

$$[a_{k\uparrow}, \sum_{k\sigma} \epsilon_k a_{k\sigma}^\dagger a_{k\sigma}] = \sum_{k\sigma} \epsilon_k [a_{k\uparrow}, a_{k\sigma} a_{k\sigma}^\dagger] \quad (3.3.16)$$

$$[a_{k\uparrow}, \sum_{k\sigma} \epsilon_k a_{k\sigma} a_{k\sigma}^\dagger] = \sum_{k\sigma} \epsilon_k (\{a_{k\uparrow}, a_{k\sigma}^\dagger\} a_{k\sigma} - \{a_{k\uparrow}, a_{k\sigma}\} a_{k\sigma}^\dagger) \quad (3.3.17)$$

$$[a_{k\uparrow}, \sum_{k\sigma} \epsilon_k a_{k\sigma}^\dagger a_{k\sigma}] = \sum_{k\sigma} \epsilon_k (\delta_{kk} \delta_{\uparrow\sigma} - 0) a_{k\sigma} \quad (3.3.18)$$

$$[a_{k\uparrow}, \sum_{k\sigma} \epsilon_k a_{k\sigma} a_{k\sigma}^\dagger] = \epsilon_k a_{k\uparrow} \quad (3.3.19)$$

again let us do the second term

$$[a_{k\uparrow}, - \sum_{k,k'} v_{k,k'} a_{k'\downarrow} a_{-k'\uparrow} a_{k\uparrow}^\dagger a_{-k\downarrow}^\dagger] = - \sum_{k,k'} v_{k,k'} [a_{k\uparrow}, a_{k'\downarrow} a_{-k'\uparrow} a_{k\uparrow}^\dagger a_{-k\downarrow}^\dagger] \quad (3.3.20)$$

$$[a_{k\uparrow}, -\sum_{k,k'} v_{k,k'} a_{k'\downarrow} a_{-k'\uparrow} a_{k\uparrow}^\dagger a_{-k\downarrow}^\dagger] = -\sum_{k,k'} v_{k,k'} (\{a_{k\uparrow}, a_{k'\downarrow} a_{-k'\uparrow}\} a_{k\uparrow}^\dagger a_{-k\downarrow}^\dagger - \{a_{k\uparrow}, a_{k\uparrow}^\dagger a_{-k\downarrow}^\dagger\} a_{k'\downarrow} a_{-k'\uparrow}) \quad (3.3.21)$$

$$[a_{k\uparrow}, -\sum_{k,k'} v_{k,k'} a_{k\uparrow}^\dagger a_{-k\downarrow}^\dagger a_{k'\downarrow} a_{-k'\uparrow}] = -\sum_{k,k'} v_{k,k'} \delta_{kk'} \delta_{\uparrow\uparrow} a_{-k\downarrow}^\dagger a_{k'\downarrow} a_{-k'\uparrow} \quad (3.3.22)$$

$$[a_{k\uparrow}, -\sum_{k,k'} v_{k,k'} a_{k\uparrow}^\dagger a_{-k\downarrow}^\dagger a_{k'\downarrow} a_{-k'\uparrow}] = -v \sum_{k,k'} a_{-k\downarrow}^\dagger a_{k'\downarrow} a_{-k'\uparrow} \quad (3.3.23)$$

and let us do

$$[a_{k\uparrow}, \sum_{k,q,l,l'} \alpha_{k,q} (a_{k\uparrow}^\dagger a_{-k\downarrow}^\dagger b_l b_{l'} + h.c)] \quad (3.3.24)$$

$$\sum_{k,q,l,l'} \alpha_{k,q} ([a_{k\uparrow}, a_{k\uparrow}^\dagger a_{-k\downarrow}^\dagger b_l b_{l'} + h.c)] \quad (3.3.25)$$

$$\sum_{k,q,l,l'} \alpha_{k,q} ([a_{k\uparrow}, a_{k\uparrow}^\dagger a_{-k\downarrow}^\dagger b_l b_{l'} + h.c)] \quad (3.3.26)$$

where $h.c = b_{l\uparrow}^\dagger b_{l'\downarrow}^\dagger a_{k\uparrow} a_{-k\downarrow}$

$$\sum_{k,q,l,l'} \alpha_{k,q} ([a_{k\uparrow}, a_{k\uparrow}^\dagger a_{-k\downarrow}^\dagger b_l b_{l'}] + [a_{k\uparrow}, b_{l\uparrow}^\dagger b_{l'\downarrow}^\dagger a_{k\uparrow} a_{-k\downarrow}]) \quad (3.3.27)$$

from this let us do the first term.

$$\sum_{k,q,l,l'} \alpha_{k,q} [a_{k\uparrow}, a_{k\uparrow}^\dagger a_{-k\downarrow}^\dagger b_l b_{l'}] = \sum_{k,q,l,l'} \alpha_{k,q} (\{a_{k\uparrow}, a_{k\uparrow}^\dagger\} a_{-k\downarrow} - \{a_{k\uparrow}, a_{-k\downarrow}^\dagger\}) b_l b_{l'} \quad (3.3.28)$$

$$\sum_{k,q,l,l'} \alpha_{k,q} [a_{k\uparrow}, a_{k\uparrow}^\dagger a_{-k\downarrow}^\dagger] b_l b_{l'} = \sum_{k,q,l,l'} \alpha_{k,q} (\delta_{kk} \delta_{\uparrow\uparrow} a_{-k\downarrow} - \delta_{k(-k)} \delta_{\uparrow\downarrow} a_{k\uparrow}) b_l b_{l'} \quad (3.3.29)$$

$$\sum_{k,q,l,l'} \alpha_{k,q} [a_{k\uparrow}, a_{k\uparrow}^\dagger a_{-k\downarrow}^\dagger] b_l b_{l'} = \sum_{k,q,l,l'} \alpha_{k,q} a_{-k\downarrow}^\dagger b_l b_{l'} \quad (3.3.30)$$

and

$$[a_{k\uparrow}, h.c] = 0 \quad (3.3.31)$$

Therefore

$$[a_{k\uparrow}, H_3] = \sum_{k,q,l,l'} \alpha_{k,q} a_{-k\downarrow}^\dagger b_l b_{l'} \quad (3.3.32)$$

by substitutting these in to the Hamiltonian then we get,

$$\langle\langle a_{k\uparrow}, a_{k'\uparrow}^\dagger \rangle\rangle = \frac{1 - (\Delta - \eta) \langle\langle a_{-k\uparrow}^\dagger, a_{k'\uparrow}^\dagger \rangle\rangle}{\omega - \epsilon_K} \quad (3.3.33)$$

One can also obtain the equation of motion for higher order Greens function.

$\langle\langle a_{-k\uparrow}^\dagger, a_{k'\uparrow}^\dagger \rangle\rangle$ which is,

$$\omega \langle\langle a_{-k\uparrow}^\dagger, a_{k'\uparrow}^\dagger \rangle\rangle = \sum_{lmp} \alpha_{lm} [a_{-k\uparrow}, a_{-p\uparrow} a_{p\uparrow}] b_{l\uparrow} b_{m\downarrow}^\dagger \quad (3.3.34)$$

$$\omega \langle\langle a_{-k\uparrow}^\dagger, a_{k'\uparrow}^\dagger \rangle\rangle = \sum_{lmp} \alpha_{lm} ([a_{-k\uparrow}, a_{-p\uparrow}] a_{p\uparrow} + [a_{-k\uparrow}, a_{p\uparrow}] a_{-p\uparrow}) b_{l\uparrow} b_{m\downarrow}^\dagger \quad (3.3.35)$$

$$\omega \langle\langle a_{-k\uparrow}^\dagger, a_{k'\uparrow}^\dagger \rangle\rangle = \sum_{lm} \alpha_{lm} (\delta_{-k-p} a_{p\uparrow} + a_{-p\uparrow} \delta_{-kp}) b_{l\uparrow} b_{m\downarrow}^\dagger \quad (3.3.36)$$

$$\omega \langle\langle a_{-k\uparrow}^\dagger, a_{k'\uparrow}^\dagger \rangle\rangle = \sum_{lm} \alpha_{lm} a_{k\uparrow} b_{l\uparrow} b_{m\downarrow}^\dagger \quad (3.3.37)$$

substituting these in to the hamiltonian then we get ,

$$\omega \langle\langle a_{-k\uparrow}^\dagger, a_{k'\uparrow}^\dagger \rangle\rangle = -\epsilon_K \langle\langle a_{-k\uparrow}^\dagger, a_{k'\uparrow}^\dagger \rangle\rangle - \sum_p v \langle a_{p\uparrow}^\dagger, a_{-p\uparrow}^\dagger \rangle \langle\langle a_{k\uparrow}, a_{k\uparrow}^\dagger \rangle\rangle + \sum_{lm} \alpha_{lm} \langle\langle a_{k\uparrow}, a_{k\uparrow}^\dagger \rangle\rangle \langle b_{l\uparrow} b_{m\downarrow}^\dagger \rangle \quad (3.3.38)$$

and

$$\langle\langle a_{k\uparrow}, a_{k'\uparrow}^\dagger \rangle\rangle = \frac{1 - (\Delta - \eta) \langle\langle a_{-k\uparrow}^\dagger, a_{k'\uparrow}^\dagger \rangle\rangle}{\omega - \epsilon_K} \quad (3.3.39)$$

$$(\omega + \epsilon_K) \langle\langle a_{-k\uparrow}^\dagger, a_{k\uparrow}^\dagger \rangle\rangle = -\frac{(1 - (\Delta - \eta))(\Delta - \eta) \langle\langle a_{-k\uparrow}^\dagger, a_{k'\uparrow}^\dagger \rangle\rangle}{\omega - \epsilon_K} \quad (3.3.40)$$

$$[(\omega + \epsilon_K) + \frac{(\Delta - \eta)^2}{\omega - \epsilon_K}] \langle\langle a_{-k\uparrow}^\dagger, a_{k'\uparrow}^\dagger \rangle\rangle = \frac{\Delta - \eta}{\omega - \epsilon_K} \quad (3.3.41)$$

$$\frac{-(\Delta - \eta)^2 + \omega^2 - \epsilon_K^2}{\omega - \epsilon_K} \langle\langle a_{-k\uparrow}^\dagger, a_{k'\uparrow}^\dagger \rangle\rangle = \frac{\Delta - \eta}{\omega - \epsilon_K} \quad (3.3.42)$$

$$\langle\langle a_{-k\uparrow}^\dagger, a_{k'\uparrow}^\dagger \rangle\rangle = \frac{-(\Delta - \eta)}{-(\Delta - \eta)^2 + \omega^2 - \epsilon_K^2} \quad (3.3.43)$$

Δ is superconducting order parameter analogue to BCS parameter.

η is magnetic ordering using the relation for Δ .

$$\Delta = -\frac{v}{\beta} \sum \langle\langle a_{-k\uparrow}^\dagger, a_{k'\uparrow}^\dagger \rangle\rangle \quad (3.3.44)$$

$$\Delta = \frac{v}{\beta} \sum_{kn} \frac{\Delta - \eta}{(\omega^2 - \epsilon_k^2) - (\Delta - \eta)^2} \quad (3.3.45)$$

and the sum may be changed into the integral by introducing the density of states.

$$N(\epsilon) = \frac{1}{v} \sum \longrightarrow \frac{1}{2\pi^3} \int d^3k = \int_{-E_f}^{\infty} dEN(E) \quad (3.3.46)$$

the summation with respect to k and n extends over all allowed pair states,therefore,

$$\Delta = \frac{1}{\beta} \sum_n \int_{-E_f}^{\infty} dEN(E) \frac{\Delta - \eta}{(\omega^2 - \epsilon_k^2) - (\Delta - \eta)^2} \quad (3.3.47)$$

attractive interaction is effective for the region $-\hbar\omega_b < E < \hbar\omega_b$ and assuming the density of states does not vary over this integral then the expression becomes,

$$\Delta = -\frac{2NEV}{\beta} \sum_n \int_0^{\hbar\omega_b} dE \left[\frac{\Delta - \eta}{(\omega^2 - \epsilon_k^2) - (\Delta - \eta)^2} \right] \quad (3.3.48)$$

Now changing $\omega=i\omega_n$

using the Matsubara frequency

$$\omega_n = i \frac{(2n+1)\pi}{\beta}$$

then the above equation becomes,

$$\Delta = 2N(0)V\beta \sum_n \int_0^{\hbar\omega_b} dE \left[\frac{\Delta - \eta}{(2n+1)^2\pi^2 + (\beta E)^2} \right] \quad (3.3.49)$$

where

$$E^2 = (\epsilon_k)^2 + (\Delta - \eta)^2$$

using the relation

$$\frac{1}{2x} \tanh \frac{x}{2} = \sum_n \frac{1}{(2n+1)^2\pi^2 + x^2}$$

then we can write the above equation as follows ,

$$\Delta = 2N(0)V\beta \int_0^{\hbar\omega_b} dE (\Delta - \eta) \frac{1}{2\beta E} \tanh \frac{\beta E}{2} \quad (3.3.50)$$

let $N(0)V = \lambda$ Then

$$\frac{\Delta}{\lambda} = \int_0^{\hbar\omega_b} dE \frac{(\Delta - \eta)}{\sqrt{(\epsilon^2 + (\Delta - \eta)^2)}} \tanh\left(\beta \frac{\sqrt{(\epsilon^2 + (\Delta - \eta)^2)}}{2}\right) \quad (3.3.51)$$

let us study the equation in different cases as

$T \rightarrow 0k$ and $T \rightarrow T_c$ as $T \rightarrow 0k$

$\beta = \infty$

one can take

$\tanh \frac{\beta E}{2} \rightarrow 1$

then the above equation becomes as follows,

$$\frac{\Delta}{\lambda} = \int_0^{\hbar\omega_b} dE \frac{(\Delta - \eta)}{\sqrt{(\epsilon^2 + (\Delta - \eta)^2)}} \quad (3.3.52)$$

using the integral $\int \frac{a}{\sqrt{(a^2+x^2)}} dx = a \arcsin \frac{x}{a}$

then the above equation becomes as,

$$\frac{1}{\lambda} = \left(1 - \frac{\eta}{\Delta}\right) \arcsin\left(\frac{\hbar\omega_b}{\Delta - \eta}\right) \quad (3.3.53)$$

$$\left(1 - \frac{\eta}{\Delta}\right) \arcsin\left(\frac{\hbar\omega_b}{\Delta - \eta}\right) = \left(1 - \frac{\eta}{\Delta}\right) \ln\left[\frac{\hbar\omega_b}{\Delta - \eta} + \sqrt{\frac{(\hbar\omega_b)^2}{(\Delta - \eta)^2} + 1}\right] \quad (3.3.54)$$

$$\left(1 - \frac{\eta}{\Delta}\right) \arcsin\left(\frac{\hbar\omega_b}{\Delta - \eta}\right) \approx \left(1 - \frac{\eta}{\Delta}\right) \ln\left[\frac{2\hbar\omega_b}{\Delta - \eta}\right] \quad (3.3.55)$$

w/c implies that

$$(\Delta - \eta) = 2\hbar\omega_b \exp \frac{-1}{\lambda\left(1 - \frac{\eta}{\Delta}\right)} \quad (3.3.56)$$

w/c is similar to BCS theory except the η and $\left(1 - \frac{\eta}{\Delta}\right)$ term. If we use $\Delta(0)$ of BCS theory at $T=0$ w/c is given by

$$2\Delta(0) = 3.5k_B T_c \quad (3.3.57)$$

for the compound $SmFeAsF_xO_{1-x}$ the experimental result of $T_c = 51.5k$ so that

$$\Delta(0) = 1.75k_B T_c = 90.125$$

At $T = 0$ the expression for η using equation(3.3.55) becomes

$$\eta = 1.75k_B T_c - 2\hbar\omega_b \exp \frac{-1}{\lambda(1 - \frac{\eta}{1.75k_B T_c})} \quad (3.3.58)$$

As $T \rightarrow T_c$ using equation (3.3.50)

$$\frac{\Delta}{\lambda} = \int_0^{\hbar\omega_b} dE \frac{(\Delta - \eta)}{\sqrt{(\epsilon^2 + (\Delta - \eta)^2)}} \tanh\left(\beta \frac{\sqrt{(\epsilon^2 + (\Delta - \eta)^2)}}{2}\right) \quad (3.3.59)$$

$$\frac{1}{\lambda} = \int_0^{\hbar\omega_b} dE \frac{(1 - \frac{\eta}{\Delta})}{\sqrt{(\epsilon^2 + (\Delta - \eta)^2)}} \tanh\left(\beta \frac{\sqrt{(\epsilon^2 + (\Delta - \eta)^2)}}{2}\right) \quad (3.3.60)$$

$$\begin{aligned} \frac{1}{\lambda} &= \int_0^{\hbar\omega_b} dE \frac{1}{\sqrt{(\epsilon^2 + (\Delta - \eta)^2)}} \tanh\left(\beta \frac{\sqrt{(\epsilon^2 + (\Delta - \eta)^2)}}{2}\right) \\ &\quad - \int_0^{\hbar\omega_b} dE \frac{\eta}{\Delta \sqrt{(\epsilon^2 + (\Delta - \eta)^2)}} \tanh\left(\beta \frac{\sqrt{(\epsilon^2 + (\Delta - \eta)^2)}}{2}\right) \end{aligned} \quad (3.3.61)$$

At $T = T_c, \Delta = 0$

The first integral of equation (3.3.60) becomes as

$$\int_0^{\hbar\omega_b} dE \frac{1}{\sqrt{(\epsilon^2 + (\Delta - \eta)^2)}} \tanh\left(\beta \frac{\sqrt{(\epsilon^2 + (\Delta - \eta)^2)}}{2}\right) = \int_0^{\hbar\omega_b} dE \frac{2}{\beta} \sum_{n=-\infty}^{\infty} \frac{1}{\omega_n^2 + E^2 + \eta^2} \quad (3.3.62)$$

using laplace transform and Matsubara frequency

$\omega_n = (2n + 1)\frac{\pi}{\beta}$ then the above integral becomes

$$\int_0^{\hbar\omega_b} dE \frac{1}{\sqrt{(\epsilon^2 + (\Delta - \eta)^2)}} \tanh\left(\beta \frac{\sqrt{(\epsilon^2 + (\Delta - \eta)^2)}}{2}\right) = \int_0^{\hbar\omega_b} dE \frac{2}{\beta} \sum_{n=-\infty}^{\infty} \frac{1}{\omega_n^2 + E^2 + \eta^2} \quad (3.3.63)$$

$$\int_0^{\hbar\omega_b} dE \frac{1}{\sqrt{(\epsilon^2 + (\Delta - \eta)^2)}} \tanh\left(\beta \frac{\sqrt{(\epsilon^2 + (\Delta - \eta)^2)}}{2}\right) = \int_0^{\hbar\omega_b} dE \frac{2}{\beta} \sum_{n=-\infty}^{\infty} \frac{1}{\omega_n^2 + E^2} \quad (3.3.64)$$

$$- \int_0^{\hbar\omega_b} dE \eta^2 \frac{2}{\beta} \sum_{n=-\infty}^{\infty} \frac{1}{\omega_n^2 + E^2} + \dots$$

$$\int_0^{\hbar\omega_b} dE \frac{2}{\beta} \sum_{n=-\infty}^{\infty} \frac{1}{\omega_n^2 + E^2} - \int_0^{\hbar\omega_b} dE \eta^2 \frac{2}{\beta} \sum_{n=-\infty}^{\infty} \frac{1}{\omega_n^2 + E^2} + \dots = \int_0^{\hbar\omega_b} dE \frac{\tanh \frac{\beta\epsilon}{2}}{\epsilon} \quad (3.3.65)$$

$$- \int_0^{\hbar\omega_b} dE \frac{2}{\beta} \sum_{n=-\infty}^{\infty} \frac{\beta^2}{((2n + 1)^2 \pi^2 + E^2 \beta^2)^2} + \dots$$

but

$$\begin{aligned} \sum_{n=-\infty}^{\infty} \frac{\beta^2}{((2n+1)^2\pi^2 + E^2\beta^2)^2} &= 2 \sum_{n=0}^{\infty} \frac{\beta^2}{((2n+1)^2\pi^2 + E^2\beta^2)^2} \\ 2 \sum_{n=0}^{\infty} \frac{1}{(a^2 + E^2)^2} &= 2 \sum_{n=0}^{\infty} \frac{1}{a^4(1 + \frac{E^2}{a^2})} = 2 \sum_{n=0}^{\infty} \frac{1}{a^4(1+x^2)} \end{aligned}$$

Where $x^2 = \frac{E^2}{a^2}$

Then

$$\sum_{n=0}^{\infty} \frac{1}{\sqrt{E^2 + \eta^2}} \tanh\left(\beta \frac{\sqrt{E^2 + \eta^2}}{2}\right) = \int_0^{\hbar\omega_b} dE \frac{\tanh \frac{\beta\epsilon}{2}}{\epsilon} - \int_0^{\hbar\omega_b} dE \eta^2 \frac{4}{\beta} \sum_{n=0}^{\infty} \frac{1}{a^4(1+x^2)} \quad (3.3.66)$$

$$\sum_{n=0}^{\infty} \frac{1}{\sqrt{E^2 + \eta^2}} \tanh\left(\beta \frac{\sqrt{E^2 + \eta^2}}{2}\right) = I_1 + I_2$$

where $I_1 = \int_0^{\hbar\omega_b} dE \frac{\tanh \frac{\beta\epsilon}{2}}{\epsilon} = \int_0^{\frac{\hbar\omega_b\beta}{2}} dy \frac{\tanh(y)}{y}$

$$y = \frac{\beta E}{2}$$

$$I_1 = \ln y \tanh y \Big|_0^{\frac{\hbar\omega_b\beta}{2}} - \int_0^{\frac{\hbar\omega_b\beta}{2}} dy \frac{\ln y}{\cosh^2 y}$$

for low temperature

$$\tanh\left(\frac{\hbar\omega}{2k_B T}\right) \longrightarrow 1$$

$$I_2 = - \int_0^{\hbar\omega_b} dE \eta^2 \frac{4}{\beta} \sum_{n=0}^{\infty} \frac{1}{a^4(1+x^2)}$$

$$I_1 = \ln \frac{\beta \hbar\omega_b}{2} - \ln \frac{\pi}{4} \exp(-c) = \ln 1.14 \frac{\hbar\omega_b}{k_B T} \quad (3.3.67)$$

and

$$I_2 = - \int_0^{\hbar\omega_b} dE \eta^2 \frac{4}{\beta} \sum_{n=0}^{\infty} \frac{1}{a^4(1+x^2)} + \dots \quad (3.3.68)$$

$$I_2 = 4\eta^2 \sum_0^{\infty} \left(\frac{\beta}{\pi(2n+1)}\right)^3 \int_0^{\infty} \frac{1}{(1+x^2)^2} dx + \dots \quad (3.3.69)$$

$$I_2 \approx \frac{4\beta^2\eta^2(7)\zeta(3)\pi}{32\pi^3}$$

$$I_2 = \left(\frac{\eta}{\pi k_B T_c}\right)^2 \frac{8.414}{8} + \dots \quad (3.3.70)$$

with the use of $\int_0^{\infty} dx \frac{1}{(1+x^2)^2} = \frac{\pi}{4}$ and

$$p = 3\zeta(3) = 1.2021 \quad \zeta \text{ is a zeta function}$$

equation(3.3.64)using equation(3.3.65) and equation(3.3.68) becomes the first integral

$$\int_0^{\hbar\omega_b} dE \frac{1}{\sqrt{\epsilon k^2 + (\Delta - \eta)^2}} \tanh \beta \frac{\sqrt{(\epsilon_k^2 + (\Delta - \eta)^2)}}{2} = \ln 1.14 \frac{\hbar\omega_b}{k_B T_c} - \eta^2 \left(\frac{1}{\pi k_B T_c}\right)^2 \frac{8.414}{8} \quad (3.3.71)$$

The second integral of equation(3.3.60) applying l' Hopitals rule (differentiating the numerator and denominator),

$$I = \int_0^{\hbar\omega_b} [dE \frac{\eta}{\Delta\sqrt{(\epsilon_k^2 + (\Delta - \eta)^2)}} \tanh(\beta \frac{\sqrt{(\epsilon_k^2 + (\Delta - \eta)^2)}}{2})] \quad (3.3.72)$$

$$I = \int_0^{\hbar\omega_b} [dE \frac{\eta}{\Delta\sqrt{(\epsilon_k^2 + (\Delta - \eta)^2)}} \tanh(\beta \frac{\sqrt{(\epsilon_k^2 + (\Delta - \eta)^2)}}{2})]' \quad (3.3.73)$$

$$I = - \int_0^{\hbar\omega_b} dE \eta^2 \beta \frac{(1 - \tanh^2) \frac{\beta\sqrt{\epsilon_k^2 + (\eta)^2}}{2}}{2(\sqrt{\epsilon_k^2 + (\eta)^2})} \quad (3.3.74)$$

combining the first and the second integral result gives

$$\frac{1}{\lambda} = \ln 1.14 \frac{\hbar\omega_b}{k_B T} - (\frac{\eta}{\pi k_B T_c})^2 \frac{8.414}{8} + \int_0^{\hbar\omega_b} dE \eta^2 \beta \frac{(1 - \tanh^2) \frac{\beta\sqrt{\epsilon_k^2 + (\eta)^2}}{2}}{2(\epsilon_k^2 + (\eta)^2)} \quad (3.3.75)$$

$$\frac{1}{\lambda} = \ln 1.14 \frac{\hbar\omega_b}{k_B T} - (\frac{\eta}{\pi k_B T_c})^2 \frac{8.414}{8} + \int_0^{\hbar\omega_b} dE \eta^2 \frac{\frac{\beta\sqrt{\epsilon_k^2 + (\eta)^2}}{2}}{2k_B T_c (\epsilon_k^2 + (\eta)^2)} - \int_0^{\hbar\omega_b} dE \eta^2 \frac{\tanh^2 \frac{\beta\sqrt{\epsilon_k^2 + (\eta)^2}}{2}}{2k_B T_c (\epsilon_k^2 + (\eta)^2)} \quad (3.3.76)$$

with the use of the relation $1/\sinh^2 x = 1 - \tanh^2 x$ The result of the third term from rhs of equation(3.3.74) is

$$\int_0^{\hbar\omega_b} dE \eta^2 \frac{\frac{\beta\sqrt{\epsilon_k^2 + (\eta)^2}}{2}}{2k_B T_c (\epsilon_k^2 + (\eta)^2)} = \frac{\eta^2}{2k_B T_c} \arctan \frac{(\hbar\omega_b)}{(\eta)} = \frac{\eta^2}{4k_B T_c} \ln \left[\frac{(\eta + \hbar\omega_b)}{(\eta - \hbar\omega_b)} \right] \quad (3.3.77)$$

And the fourth term rhs of equation(3.3.74) can be integrated with FORTRAN language using the following approximation.

$$\hbar\omega_b \approx \hbar\omega_D = 10^{-3} ev \text{ for BCS}$$

and using superconducting critical temperature

$$SmAsFeF_xO_{1-x} T_C = 51.5k$$

$$\text{so } \frac{\hbar\omega_b}{2k_B T_c} \approx 0.000001$$

using $\eta = .05 - 7$ and $k_B = 1$ with the aforementioned method and the above approximation we obtain

$$\int_{10^{-10}}^{.000001} \frac{\tanh^2(.01\sqrt{(x^2 + a^2)})}{2(x^2 + a^2)} dx \approx 7.6x10^{-20} \quad (3.3.78)$$

substituting equation(3.3.75) and equation(3.3.76) in equation(3.3.74) and simplifying gives that

$$\frac{1}{\lambda} = \ln\left(1.14\frac{\hbar\omega_b}{k_B T_c}\right) - \left(\frac{\eta}{\pi k_B T_c}\right)^2 \frac{8.414}{8} + \frac{\eta}{4k_B T_c} \ln\left[\frac{(\eta + \hbar\omega_b)}{(\eta - \hbar\omega_b)}\right] \quad (3.3.79)$$

for small η we can ignore the η^2 term then equation(3.3.78) becomes,

$$\frac{1}{\lambda} = \ln\left(1.14\frac{\hbar\omega_b}{k_B T_c}\right) + \frac{\eta}{4k_B T_c} \ln\left[\frac{(\eta + \hbar\omega_b)}{(\eta - \hbar\omega_b)}\right] \quad (3.3.80)$$

$$k_B T_c = 1.14\hbar\omega_b \exp\left(-\left(\frac{1}{\lambda - a\eta}\right)\right) \quad (3.3.81)$$

$$T_c = \frac{1.14\hbar\omega_b}{k_B} \exp\left(-\left(\frac{1}{\lambda - a\eta}\right)\right) \quad (3.3.82)$$

where

$$\frac{\hbar\omega_b}{k_B} = 170k$$

$$\lambda = 0.3 - 0.9$$

$$\eta = .05 - 7$$

$$a = \frac{1}{4k_B T_c} \ln\left[\frac{(\eta + \hbar\omega_b)}{(\eta - \hbar\omega_b)}\right] = 0.00000067$$

these are taken from the experimental data.

By substituting these values into the above equation we can calculate the theoretical value for the critical temperature for

$$SmFeAs(O_{.85}F_{.15}), T_c = 55.5k$$

compound	λ_{el}	experimental $T_c(K)$	theoretical $T_c(K)$
$SmFeAsO_{.85}F_{.15}$	0.9	51.5	55.5

Table 3.1:

3.3.3 For localized electrons

The equation of motion using Greens function technique for localize electrons is as follows.

$$\omega \langle \langle b_{l\uparrow}, b_{l\uparrow}^\dagger \rangle \rangle = 1 + \langle \langle [b_{l\uparrow}, H] \rangle \rangle_\omega \quad (3.3.83)$$

Now let we first evaluate the commutation $[b_{l\uparrow}, H]$, using the hamiltonian given at the beginning of this chapter.

$$[b_{l\uparrow}, H_1] = \sum_{k\sigma} \epsilon_k [b_{l\uparrow}, a_{k\sigma} a_{k\sigma}^\dagger] + \sum_{p\sigma} \epsilon_p [b_{l\uparrow}, b_{p\sigma} b_{p\sigma}^\dagger] = 0 + \sum_{p\sigma} \epsilon_p [b_{l\uparrow}, b_{p\sigma} b_{p\sigma}^\dagger] \quad (3.3.84)$$

$$[b_{l\uparrow}, H_1] = \sum_{p\sigma} \epsilon_p (\{b_{l\uparrow}, b_{p\sigma}^\dagger\} b_{p\sigma} - b_{p\sigma}^\dagger \{b_{l\uparrow}, b_{p\sigma}\}) \quad (3.3.85)$$

$$[b_{l\uparrow}, H_1] = \sum_{p\sigma} \epsilon_p \delta_{lp} \delta_{\uparrow\sigma} b_{p\sigma} \quad (3.3.86)$$

$$[b_{l\uparrow}, H_1] = \sum_p \epsilon_p \delta_{lp} b_{p\uparrow} \quad (3.3.87)$$

$$[b_{l\uparrow}, H_1] = \epsilon_l b_{l\uparrow} \quad (3.3.88)$$

Again let us do the commutation

$$[bl\uparrow, H_2] = 0$$

so the remaining is

$$[bl\uparrow, H_3] = \sum_{lm} \alpha_{lm} [b_{l\uparrow}, a_{k\uparrow}^\dagger a_{-k\uparrow}^\dagger b_{l\uparrow} b_{m\downarrow}] + \sum_{lmp} \alpha_{lm}^* [bl\uparrow, a_{k\uparrow} a_{-k'\uparrow} b_{p\uparrow}^\dagger b_{m\downarrow}^\dagger] \quad (3.3.89)$$

$$[bl\uparrow, H_3] = 0 + \sum_{lmp} \alpha_{lm}^* [bl\uparrow, a_{k\uparrow} a_{-k\uparrow} b_{p\uparrow}^\dagger b_{m\downarrow}^\dagger] \quad (3.3.90)$$

$$[bl\uparrow, H_3] = \sum_{lmp} \alpha_{lm}^* a_{k\uparrow} a_{-k'\uparrow} [bl\uparrow, b_{p\uparrow}^\dagger b_{m\downarrow}^\dagger] \quad (3.3.91)$$

$$[bl\uparrow, H_3] = \sum_{lmp} \alpha_{lm}^* a_{k\uparrow} a_{-k'\uparrow} (\{bl\uparrow, b_{p\uparrow}^\dagger\} b_{m\downarrow}^\dagger - b_{p\uparrow}^\dagger \{b_{l\uparrow}, b_{m\downarrow}^\dagger\}) \quad (3.3.92)$$

$$[bl \uparrow, H_3] = \sum_{lmp} \alpha_{lm}^* a_{k\uparrow} a_{-k\uparrow} (\delta_{lp} b_{m\downarrow}^\dagger - \delta_{lm} b_{p\uparrow}^\dagger) \quad (3.3.93)$$

$$[bl \uparrow, H_3] = \sum_{lm} \alpha_{lm} a_{k\uparrow} a_{-k\uparrow} b_{m\downarrow}^\dagger \quad (3.3.94)$$

Where $\alpha = \alpha^*$ substituting equation(3.3.85) and equation(3.3.91) into equation(3.3.80) yields

$$\omega \langle \langle b_{l\uparrow}, b_{l\uparrow}^\dagger \rangle \rangle = 1 + \epsilon_l \langle \langle b_{l\uparrow}, b_{l\uparrow}^\dagger \rangle \rangle + \sum_{lm} \alpha_{lm} \langle a_{k\uparrow} a_{-k'\uparrow}, a_{-k\uparrow} \rangle \langle \langle b_{m\downarrow}^\dagger, b_{l\uparrow}^\dagger \rangle \rangle \quad (3.3.95)$$

$$(\omega - \epsilon_l) \langle \langle b_{l\uparrow}, b_{l\uparrow}^\dagger \rangle \rangle = 1 + \Delta_l \langle \langle b_{m\downarrow}^\dagger, b_{l\uparrow}^\dagger \rangle \rangle \quad (3.3.96)$$

This implies that

$$\langle \langle b_{l\uparrow}, b_{l\uparrow}^\dagger \rangle \rangle = \frac{1}{\omega - \epsilon_l} + \frac{\Delta_l \langle \langle b_{m\downarrow}^\dagger, b_{l\uparrow}^\dagger \rangle \rangle}{\omega - \epsilon_l} \quad (3.3.97)$$

where $\Delta_l = \sum_{lm} \alpha_{lm} a_{k\uparrow} a_{-k'\uparrow}$ one can obtain the equation of motion for higher order Green's function $\langle \langle b_{m\downarrow}^\dagger, b_{l\uparrow}^\dagger \rangle \rangle$ using

$$\omega \langle \langle b_{m\downarrow}^\dagger, b_{l\uparrow}^\dagger \rangle \rangle = \langle [b_{m\downarrow}^\dagger, b_{l\uparrow}^\dagger] \rangle + \langle \langle [b_{m\downarrow}^\dagger, H], b_{l\uparrow}^\dagger \rangle \rangle \quad (3.3.98)$$

$$\omega \langle \langle b_{m\downarrow}^\dagger, b_{l\uparrow}^\dagger \rangle \rangle = 0 + \langle \langle [b_{m\downarrow}^\dagger, H], b_{l\uparrow}^\dagger \rangle \rangle \quad (3.3.99)$$

using the same techniques as in the above,

$$[b_{m\uparrow}, H_1] = \sum_{k\sigma} \epsilon_k [b_{m\downarrow}^\dagger, a_{k\sigma}^\dagger a_{k\sigma}] + \sum_{l\sigma} \epsilon_l [b_{m\downarrow}^\dagger, b_{l\sigma}^\dagger b_{l\sigma}] \quad (3.3.100)$$

$$[b_{m\uparrow}, H_1] = 0 + \sum_{l\sigma} \epsilon_l [b_{m\downarrow}^\dagger, b_{l\sigma}^\dagger b_{l\sigma}] \quad (3.3.101)$$

$$[b_{m\downarrow}, H_1] = \sum_{l\sigma} \epsilon_l (\{b_{m\downarrow}^\dagger, b_{l\sigma}^\dagger\} b_{l\sigma} - b_{l\sigma}^\dagger \{b_{m\downarrow}^\dagger, b_{l\sigma}\}) \quad (3.3.102)$$

$$[b_{m\downarrow}, H_1] = - \sum_{l\sigma} \epsilon_l b_{l\sigma}^\dagger \delta_{ml} \quad (3.3.103)$$

$$[b_{m\uparrow}, H_1] = -\epsilon_m b_{m\downarrow}^\dagger \quad (3.3.104)$$

The commutation

$$[b_{m\uparrow}^\dagger, H_2] = 0$$

the remaining is

$$[b_{m\downarrow}^\dagger, H_3] = \sum_{lmp} \alpha_{lm} [b_{m\downarrow}^\dagger, a_{k\uparrow}^\dagger a_{-k\uparrow}^\dagger b_{l\uparrow} b_{p\uparrow}] + \sum_{lmp} \alpha_{lmp}^* [b_{m\downarrow}^\dagger, a_{-k\uparrow} a_{k\uparrow} b_{l\uparrow}^\dagger b_{m\downarrow}^\dagger] \quad (3.3.105)$$

$$[b_{m\downarrow}^\dagger, H_3] = \sum_{lmp} \alpha_{lm} [b_{m\downarrow}^\dagger, a_{k\uparrow}^\dagger a_{-k\uparrow}^\dagger b_{l\uparrow} b_{p\uparrow}] + 0 \quad (3.3.106)$$

$$[b_{m\downarrow}^\dagger, H_3] = \sum_{lmp} \alpha_{lm} a_{k\uparrow}^\dagger a_{-k\uparrow}^\dagger [b_{m\downarrow}^\dagger, b_{l\uparrow} b_{p\uparrow}] \quad (3.3.107)$$

$$[b_{m\downarrow}^\dagger, H_3] = \sum_{lmp} \alpha_{lm} a_{k\uparrow}^\dagger a_{-k\uparrow}^\dagger (\{b_{m\downarrow}^\dagger, b_{l\uparrow}\} b_{p\uparrow} - b_{l\uparrow} \{b_{m\downarrow}^\dagger, b_{p\uparrow}\}) \quad (3.3.108)$$

$$[b_{m\downarrow}^\dagger, H_3] = \sum_{lmp} \alpha_{lm} a_{k\uparrow}^\dagger a_{-k\uparrow}^\dagger (b_{m\downarrow} \delta_{ml} - b_{l\uparrow} \delta_{mp}) \quad (3.3.109)$$

$$[b_{m\downarrow}^\dagger, H_3] = \sum_{lm} \alpha_{lm} a_{k\uparrow}^\dagger a_{-k\uparrow}^\dagger b_{l\uparrow} \quad (3.3.110)$$

substituting equation(3.3.100) and equation(3.3.106) into equation(3.3.96) and assuming $\epsilon_l = \epsilon_m$ yields that,

$$\omega \langle\langle b_{m\downarrow}^\dagger, b_{l\uparrow}^\dagger \rangle\rangle = -\epsilon_l \langle\langle b_{m\downarrow}^\dagger, b_{l\uparrow}^\dagger \rangle\rangle + \sum_{lm} \alpha_{lm} \langle a_{k\uparrow}^\dagger a_{-k\uparrow}^\dagger \rangle \langle\langle b_{l\uparrow}, b_{l\uparrow}^\dagger \rangle\rangle \quad (3.3.111)$$

$$\omega + \epsilon_l \langle\langle b_{m\downarrow}^\dagger, b_{l\uparrow}^\dagger \rangle\rangle = \Delta_l \langle\langle b_{l\uparrow}, b_{l\uparrow}^\dagger \rangle\rangle \quad (3.3.112)$$

$$\langle\langle b_{m\downarrow}^\dagger, b_{l\uparrow}^\dagger \rangle\rangle = \frac{\Delta_l \langle\langle b_{l\uparrow}, b_{l\uparrow}^\dagger \rangle\rangle}{\omega + \epsilon_l} \quad (3.3.113)$$

Now combining equation(3.3.94) and equation(3.3.109) gives the following two equations.

$$\langle\langle b_{m\downarrow}^\dagger, b_{l\uparrow}^\dagger \rangle\rangle = \frac{\Delta_l}{(\omega + \epsilon_l)(\omega - \epsilon_l)} + \frac{\Delta_l}{(\omega - \epsilon_l)} \langle\langle b_{m\downarrow}^\dagger, b_{l\uparrow}^\dagger \rangle\rangle \quad (3.3.114)$$

$$(1 - \frac{\Delta_l^2}{\omega^2 - \epsilon_l^2}) \langle\langle b_{m\downarrow}^\dagger, b_{l\uparrow}^\dagger \rangle\rangle = \frac{\Delta_l}{\omega^2 - \epsilon_l^2} \quad (3.3.115)$$

Therefore

$$\langle\langle b_{m\downarrow}^\dagger, b_{l\uparrow}^\dagger \rangle\rangle = \frac{\Delta_l}{\omega^2 - \epsilon_l^2 - \Delta_l^2} \quad (3.3.116)$$

and

$$\langle\langle b_{l\uparrow}, b_{l\uparrow}^\dagger \rangle\rangle = \frac{1}{\omega - \epsilon_l} + \frac{\Delta_l \langle\langle b_{m\downarrow}^\dagger, b_{l\uparrow}^\dagger \rangle\rangle}{\omega - \epsilon_l} \quad (3.3.117)$$

$$\left(1 - \frac{\Delta_l^2}{\omega^2 - \epsilon_l^2}\right) \langle\langle b_{l\uparrow}, b_{l\uparrow}^\dagger \rangle\rangle = \frac{1}{\omega - \epsilon_l} \quad (3.3.118)$$

This implies that

$$\langle\langle b_{l\uparrow}, b_{l\uparrow}^\dagger \rangle\rangle = \frac{\omega + \epsilon_l}{\omega^2 - \epsilon_l^2 - \Delta_l^2} \quad (3.3.119)$$

This equation shows that the correlation between conduction and mobile electrons:

from our previous definition η we can write $\eta = \frac{\alpha}{\beta} \sum_{k,n} \langle\langle b_{l\uparrow}^\dagger, b_{m\downarrow}^\dagger \rangle\rangle = \frac{\alpha}{\beta} \sum \frac{\Delta_l}{\omega^2 - \epsilon_l^2 - \Delta_l^2}$
and the sum may be changed into an integral by introducing the density of states.

$$N_E, \frac{1}{V} \sum_{k,n} \longrightarrow \frac{1}{(2\pi)^3} \int_{-\epsilon_f}^{\infty} dE N_E$$

The summation with respect to k and n extends over all allowed pair states. therefore

$$\eta = -\frac{\alpha}{\beta} \sum_n \int_{-\epsilon_f}^{\infty} dE N_E \frac{(\Delta_l)}{(\omega^2 - \epsilon_l^2 - \Delta_l^2)} \quad (3.3.120)$$

For effective attractive interaction region and assuming the density of state constant the expression becomes.

$$\eta = -2N_E \frac{\alpha}{\beta} \sum_n \int_0^{\hbar\omega_b} dE \frac{(\Delta_l)}{(\omega^2 - \epsilon_l^2 - \Delta_l^2)} \quad (3.3.121)$$

Now changing $\omega_b \longrightarrow \omega_n$ and using the matsubra frequency

$$\omega_n = \frac{(2n+1)\pi i}{\beta}$$

then equation(3.3.117) becomes

$$\eta = 2N_E \alpha \beta \sum_n \int_0^{\hbar\omega_b} dE \frac{(\Delta_l)}{((2n+1)^2 \pi^2 + E^2 \beta^2)} \quad (3.3.122)$$

Where $E^2 = \epsilon^2 + \Delta_l^2$

using the relation $\frac{1}{2x} \tanh\left(\frac{x}{2}\right) = \sum_n \frac{1}{(2n+1)^2 \pi^2 + x^2}$

we can write the above equation as follows.

$$\eta = N_E \alpha \beta \int_0^{\hbar\omega_b} dE \frac{(\Delta_l)}{(2\beta E)} \tanh\left(\frac{\beta E}{2}\right) \quad (3.3.123)$$

Let $N_0 \alpha = \lambda_l$ this implies that

$$\eta = \lambda_l \int_0^{\hbar\omega_b} dE \frac{(\Delta_l)}{\sqrt{(\epsilon^2 + \Delta_l^2)}} \tanh\left(\beta \frac{\sqrt{(\epsilon^2 + \Delta_l^2)}}{2}\right) \quad (3.3.124)$$

Applying the same techniques as equation(3.3.74) the above equation at low temperature yields.

$$\eta = \lambda_l \Delta_l \left(\ln \left(1.14 \frac{\hbar \omega_b}{k_B T_m} \right) - \Delta_l^2 \frac{1}{(\pi k_B T_m)^2} \frac{8.414}{8} \right) \quad (3.3.125)$$

since Δ is very small we can ignore the second term

$$\eta = \lambda_l \Delta_l \ln \left(1.14 \frac{\hbar \omega_b}{k_B T_m} \right) \quad (3.3.126)$$

This implies that

$$k_B T_m = 1.14 \hbar \omega_b \exp \left(\frac{\eta}{\lambda_l \Delta_l} \right) \quad (3.3.127)$$

3.3.4 For Pure Superconducting System

For pure superconducting system (when magnetic order cannot appear or magnetic effect is zero) we can ignore the η term and our previous calculation gives the following results which is similar to BCS theory. using equation(3.3.51) as $T \rightarrow 0$ $\eta \rightarrow 0$ and $\tanh(\frac{\beta E}{2}) \rightarrow 1$ so the equation reduces to

$$\frac{\Delta}{\lambda} = \int_0^{\hbar \omega_b} d\epsilon_k \frac{\Delta_l}{\sqrt{\epsilon_k^2 + \Delta_l^2}} \quad (3.3.128)$$

$$\frac{1}{\lambda} = \int_0^{\hbar \omega_b} d\epsilon_k \frac{1}{\sqrt{\epsilon_k^2 + \Delta_l^2}} = \sinh^{-1} 1 \left(\frac{\hbar \omega_b}{\Delta_l} \right) \quad (3.3.129)$$

and as $T \rightarrow T_c$ using the same equation(3.3.51)for $\eta = 0$

$$\frac{1}{\lambda} = \int_0^{\hbar \omega_b} d\epsilon_k \tanh \frac{(\frac{\beta \epsilon_k}{2})}{\epsilon_k} \quad (3.3.130)$$

$$\frac{1}{\lambda} = \int_0^{\frac{\beta \hbar \omega_b}{2}} dy \frac{\tanh y}{y} \quad (3.3.131)$$

$$y = \frac{\beta \epsilon_k}{2}$$

$$\frac{1}{\lambda} = \ln y \tanh y \Big|_0^{\frac{\beta \hbar \omega_b}{2}} - \int_0^{\frac{\beta \hbar \omega_b}{2}} dy \frac{\ln y}{\cosh^2 y} \quad (3.3.132)$$

for low temprature $\tanh(\frac{\hbar \omega_b}{2k_B T}) \rightarrow 1$

$$\frac{1}{\lambda} \ln \left(\frac{\beta \hbar \omega_b}{2} \right) - \ln \left(\frac{\pi}{4} \right) \exp -c = \ln \left(1.14 \frac{\hbar \omega_b}{k_B T_c} \right) \quad (3.3.133)$$

$$k_B T_c = 1.14 \hbar \omega_b \exp^{-\left(\frac{1}{\lambda}\right)} \quad (3.3.134)$$

To obtain temperature dependent energy gap of equation(3.3.51) we used the same technique to solve the first integral of equation(3.3.60) which is

$$\frac{1}{\lambda} = \int_0^{\hbar \omega_b} dE \frac{1}{\sqrt{(\epsilon^2 + (\Delta - \eta)^2)}} \tanh\left(\beta \frac{\sqrt{(\epsilon^2 + (\Delta - \eta)^2)}}{2}\right) \quad (3.3.135)$$

$$\frac{1}{\lambda} = \ln\left(1.14 \frac{\hbar \omega_b}{k_B T}\right) - \Delta^2 \frac{1}{(\pi k_B T)^2} \frac{8.414}{8} + \dots \quad (3.3.136)$$

but for BCST = T_c

$\frac{1}{\lambda} = \ln\left(1.14 \frac{\hbar \omega_b}{k_B T_c}\right)$ and assuming the above equations yields that

$$\ln\left(\frac{T}{T_c}\right) = -\Delta^2 \frac{1}{(\pi k_B T)^2} \frac{8.414}{8} + \dots \quad (3.3.137)$$

using $\ln(1 - x) = -x - \frac{x^2}{2} + \dots$

implies

$$\ln\left(1 - \left(1 - \frac{T}{T_c}\right)\right) = -\left(1 - \frac{T}{T_c}\right) - \frac{1}{2}\left(1 - \frac{T}{T_c}\right)^2 + \dots$$

$$\ln\left(\frac{T}{T_c}\right) \approx -\left(1 - \frac{T}{T_c}\right)$$

implies

$$-\left(1 - \frac{T}{T_c}\right) \approx -\Delta^2 \frac{1}{(\pi k_B T)^2} \frac{8.414}{8}$$

Hence

$$\Delta_{sc}(T) = 3.06 k_B T_c \left(1 - \frac{T}{T_c}\right)^{1/2} \quad (3.3.138)$$

Chapter 4

Result and Discussion

In this chapter, we described the effect of temperature (T) on superconducting order parameter $\Delta(T)$. We also examined the effect of magnetic order parameter η on superconducting transition temperature (T_c) and on AFM transition temperature (T_m) in $SmO_{1-x}F_xFeAs$. In chapter three, using the model of the Hamiltonian and retarded double time temperature dependent Greens function formalism, we obtained mathematical expressions for superconducting transition(critical) temperature T_c , the superconducting order parameter $\Delta(T)$, the magnetic order parameter(η), and Antiferromagnetism transition temperature (T_m). From Eq. (3.3.123) we have got the superconducting transition (critical) temperature for the superconductor $SmO_{1-x}F_xFeAs$. Using this T_c value and Eq. (3.3.136), we plot the phase diagram of $\Delta(T)$ versus $T(k)$ which is shown in Figure 4.1. As seen in this figure, when the temperature increases the superconducting order parameter decreases and vanishes as the temperature is equal to the critical temperature. Based on Eq.(3.3.136) we plotted the phase diagram of T_c versus η (Fig 4.2). This figure indicates, as the magnetic order parameter (η) increases the superconducting transition temperature (T_c) decreases. The phase diagram of magnetic ordering temperature (T_m) versus magnetic ordering (η) also plotted (Fig 4.3) based on the Eq.(3.3.125). As we observed from this graph the magnetic transition temperature is increases (directly proportional) as the magnetic order parameter increases. And finally, we merged Fig

(4.2) and Fig (4.3), to indicate the region where both orders i.e.superconductivity and Antiferromagnetism are coexist.

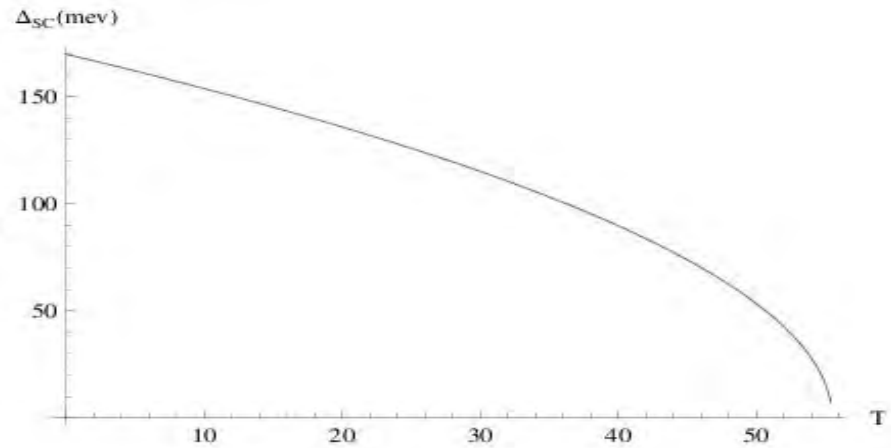


Figure 4.1: Superconducting order parameter vs. temperature for pure $SmO_{1-x}F_xFeAs$ superconductor.

As seen in fig-4.1, when the temperature increases the superconducting order parameter decreases and vanishes as the temperature is equal to the critical temperature.

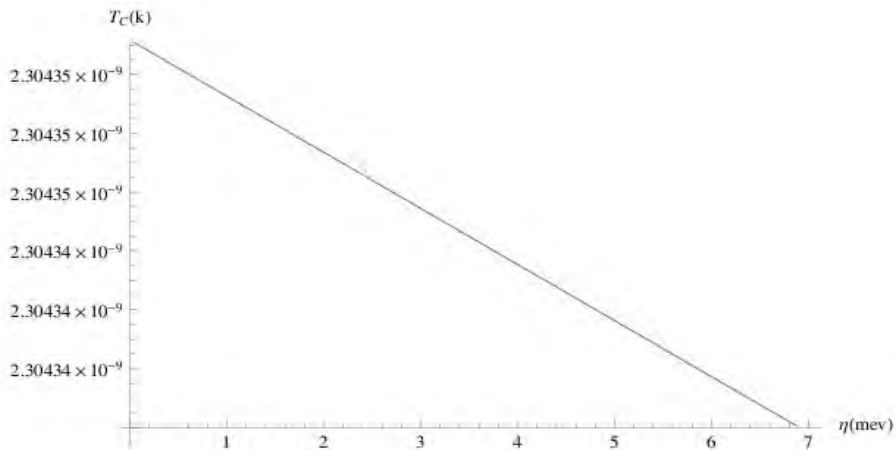


Figure 4.2: Superconducting critical temperature vs. magnetic order parameter.

Fig-4.2 indicates, as the magnetic order parameter (η) increases the superconducting transition temperature (T_c) decreases.

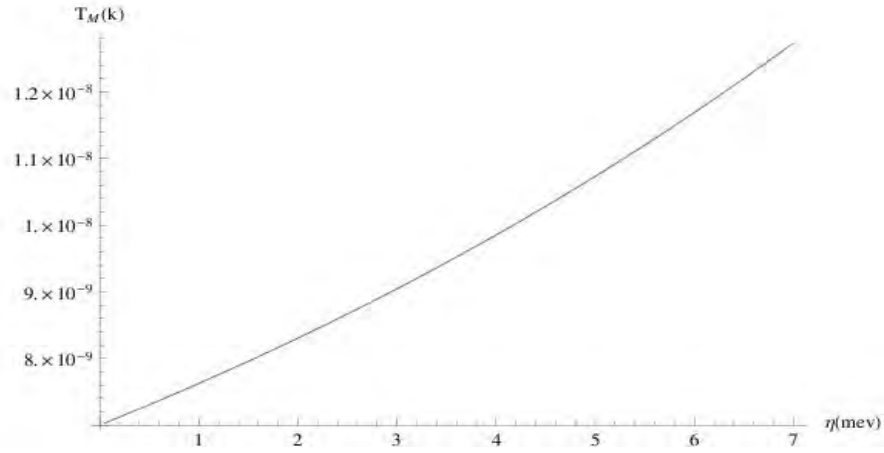


Figure 4.3: Antiferromagnetism transition temperature (T_m) vs magnetic order parameter(η).

Fig-4.3 shows that the magnetic transition temperature increases as the magnetic order parameter increases.

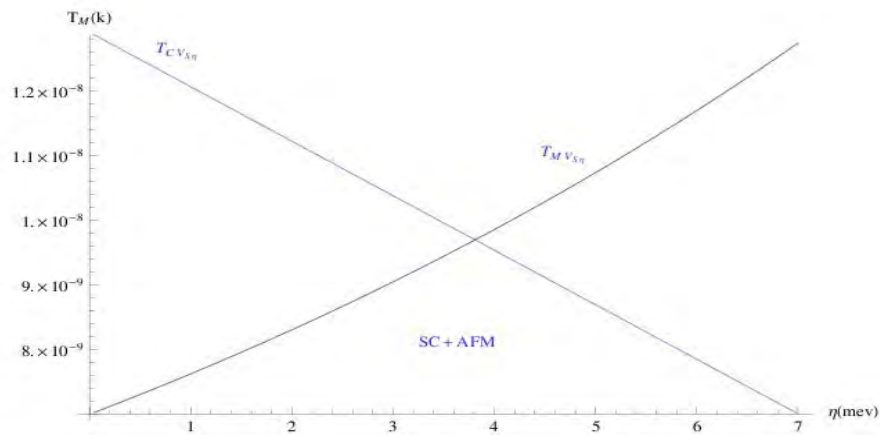


Figure 4.4: the superconducting critical temperature and AFM transition temperature vs. magnetic order parameter.

Fig-4.4 shows that the coexistence of superconductivity and AFM in $SmO_{1-x}F_xFeAs$.

Chapter 5

Conclusion

In this work, we have studied the possible co-existence of Aniferromagnetism and superconductivity in $SmO_{1-x}F_xFeAs$. Using a model Hamiltonian and Greens function formalism we obtained mathematical expression for superconducting order parameter($\Delta_{sc}(T)$), magnetic order parameter (η), critical temperature (T_c), and AFM transitional temperature (T_m). Based on these mathematical expressions we plotted the three graphs $\Delta_{sc}(T)$ vs T, T_c vs (η), (T_m) vs (η) and finally the last two graphs (T_c vs (η) and T_m vs (η) were merged to obtain the coexistence of superconductivity and AFM. The result of our work described:

- a) as temperature increases superconducting order parameter decreases.
- b) when magnetic order parameter increases the critical temperature decreases.
- c) while the magnetic order parameter increases with the AFM transitional temperature.

Moreover, the region under the intersection of the two merged graphs (Fig 4.4) shows that superconductivity and AFM coexist in $SmO_{1-x}F_xFeAs$.

Reference

- [1] H. Kamerlingh Onnes, Akad. Wetenschap (Amsterdam) **14**, 113 (1911)
- [2] J G. Bednorz and K. A. Muller, Z. Phys. B **64**, 189 (1986).
- [3] J. Nagamatsu, N. Nakagawa, T. Muranaka, Y. Zenitani, and J. Akimitsu, Nature **410**, 63 (2001)
- [4] Yoichi Kamihara, Takumi Watanabe, Masahiro Hirano, and Hideo Hosono, J. Am. Chem. Soc. **130**, 3296-3297(2008)
- [5] Shigeji Fujita and Salvador Godoy, Quantum Statistical Theory of Superconductivity .Plenum press, New York (1996)
- [6] J.R. Hook and H.E. Hall, Solid State physics second Edition. John Wiley and Sons New York (1991)
- [7] Charles Kittel, *Introduction to solid State physics sixth Edition*,(John Wiley and Sons,inc. , New York)
- [8] T. Ishiguro, K.Yamaji, G.Saito, Organic Superconductors. Springer-Verlag Berlin Heidelberg
- [9]J. Bardeen, L. N. Cooper, and J. R. Schrieffer, Phys. Rev. **108**, 1175 (1957).
- [10] Michael Tinkham, *Introduction to superconductivity second edition*, John Wiley and Sons,New York (1986)
- [11] [http://en.wikipedia.org/wiki/High-temperature sup...](http://en.wikipedia.org/wiki/High-temperature_sup...)
- [12] S. Uchida, J. Phys. Soc. Jpn. 77 (2008) Suppl.C, pp.
- [13] <http://at-mel-cf.web.cern.ch/at-mel-cf/html/physicsHTS.htm>
- [14] Ren Zhi-An, Lu Wei, Yang Jie, Yi Wei , Shen Xiao-Li , Li Zheng-Cai , Che Guang-Can, Dong Xiao-Li, Sun Li-Ling, Zhou Fang, Zhao Zhong- Xian, Chin. Phys. Lett. **25**, 2215 (2008)
- [15] A. V. Chubukov, D. V. Efremov, and I. Eremin, Phys.Rev. B **78**, 134512 (2008)
- [16] Clarina de la Cruz, Q. Huang, J. W. Lynn, Jiying Li, W. Ratcliff II, J. L. Zarestky, H. A. Dai, nature **453**, 07057(2008)
- [17] Y. Kamihara, H. Hiramatsu, M. Hirano, R. Kawamura, H. Yanagi, T. Kamiya, and H. Hosono, J. Am. Chem. Soc. **128**, 10012 (2006).
- [18] Kenji ISHIDA, Yusuke NAKAI1, and Hideo HOSONO, J.Phys.Jpn.,78,062001(2009)
- [19] D. J. Singh and M.H. Du, PR, **100**, 237003 (2008)

- [20] G. F. Chen, Z. Li, D. Wu, G. Li, W. Z. Hu, J. Dong, P. Zheng, J. L. Luo, and N. L. Wang, *Phys.Rev.Lett* **100**, 247002 (2008)
- [21] Takuj Takuji Nomura, arXiv: 0811.2462v2 [cond-mat.supr-con] 13 Mar 2009
- [22] Hideo HOSONO, *J. Phys. Soc. Jpn.* **77**, 1-8 (2008)
- [23] Yoshimitsu Kohama, Yoichi Kamihara, Masahiro Hirano, Hitoshi Kawaji, Tooru Atake, and Hideo Hosono, *Phys.Rev.* **78**, 020512 (2008)
- [24] T. Kroll, S. Bonhommeau, T. Kachel, H. A. Drr, J. Werner, G. Behr, A. Koitzsch, R. Hbel, S. Leger, R. Schnfelder, A. K. Ariffin, R. Manzke, F. M. F. de Groot, J. Fink, H. Eschrig, B. Behner, and M. Knupfer, *Phys.Rev. B* **78**, 220502(R)(2008)
- [25] Haule, J. H. Shim, and G. Kotliar, arXiv:0803.1279v1[cond-mat.str-el] 9 Mar 2008
- [26] I. I. Mazin, D. J. Singh, M. D. Johannes, and M. H. Du, *Phys. Rev.Lett.* **101**, 057003(2008).
- [27] K. Kuroki, S. Onari, R. Arita, H. Usui, Y. Tanaka, H. Kontani, and H. Aoki: *Phys. Rev.Lett.* **101**, 087004 (2008)
- [28] Takatoshi NOMURA et al., *J.Phys.Soc.Jpn.* **77**, 32-35 (2008)
- [29] <http://superconductors.org/UBNews.htm>
- [30] K. Machida, *Appl. Phys. A* **35**, 193-217 (1984)
- [31] V.L.Ginzburg, *Sov.Phys.JETP* **4**, 153(1957)
- [32] Alexander B. Shick, *PhysRevB*. **65**.180509 (2002)
- [33] A. J. Drew, Ch. Niedermayer, P. J. Baker, F. L. Pratt, S. J. Blundell, T. Lancaster, R. H. Liu, G. Wu, X. H. Chen, I. Watanabe, V. K. Malik¹, A. Dubroka¹, M. Rssle¹, K.W. Kim¹, C. Baines and C. Bernhard, www.nature.com/naturematerials 22 February 2009
- [34] Soshi Takeshita, Ryosuke Kadono, Masatoshi Hiraishi, Masanori Miyazaki,
- [35] P Singh *J.superconduct.as Novel Magnetion* 24945(2011)

Declaration

This thesis is my original work, has not been presented for a degree in any other University and that all the sources of material used for the thesis have been dully acknowledged.

Name: Abera Mebrahtu

Signature:— — — — —

Place and time of submission: Addis Ababa University, June 2010

This thesis has been submitted for examination with my approval as University advisor.

Name: Prof. P. Singh

Signature:— — — — —